Atmos. Chem. Phys., 8, 3899–3917, 2008
www.atmos-chem-phys.net/8/3899/2008/
© Author(s) 2008. This work is distributed under
the Creative Commons Attribution 3.0 License.

Atmospheric Chemistry and Physics

Observations of HNO_3, ΣAN, ΣPN and NO_2 fluxes: evidence for rapid HO_x chemistry within a pine forest canopy

D. K. Farmer[1] **and R. C. Cohen**[1,2,3]

[1]Department of Chemistry, University of California Berkeley, Berkeley, CA, USA
[2]Department of Earth and Planetary Science, University of California Berkeley, Berkeley, CA 94720, USA
[3]Energy and Environment Technologies Division, Lawrence Berkeley National Laboratory, Berkeley, CA 94720, USA

Received: 4 April 2007 – Published in Atmos. Chem. Phys. Discuss.: 24 May 2007
Revised: 19 June 2008 – Accepted: 19 June 2008 – Published: 22 July 2008

Abstract. Measurements of exchange of reactive nitrogen oxides between the atmosphere and a ponderosa pine forest in the Sierra Nevada Mountains are reported. During winter, we observe upward fluxes of NO_2, and downward fluxes of total peroxy and peroxy acyl nitrates (ΣPNs), total gas and particle phase alkyl and multifunctional alkyl nitrates ($\Sigma ANs_{(g+p)}$), and the sum of gaseous HNO_3 and semi-volatile NO_3^- particles ($HNO_{3(g+p)}$). We use calculations of the vertical profile and flux of NO, partially constrained by observations, to show that net midday ΣNO_{yi} fluxes in winter are –4.9 ppt m s^{-1}. The signs and magnitudes of these wintertime individual and ΣNO_{yi} fluxes are in the range of prior measurements. In contrast, during summer, we observe downward fluxes only of $\Sigma ANs_{(g+p)}$, and upward fluxes of $HNO_{3(g+p)}$, ΣPNs and NO_2 with signs and magnitudes that are unlike most, if not all, previous observations and analyses of fluxes of individual nitrogen oxides. The results imply that the mechanisms contributing to NO_y fluxes, at least at this site, are much more complex than previously recognized. We show that the observations of upward fluxes of $HNO_{3(g+p)}$ and ΣPNs during summer are consistent with oxidation of NO_2 and acetaldehyde by an OH x residence time of 1.1×10^{10} molec OH cm^{-3} s, corresponding to 3 to 16×10^7 molecules cm^{-3} OH within the forest canopy for a 420 to 70 s canopy residence time. We show that $\Sigma AN_{(g+p)}$ fluxes are consistent with this range in OH if the reaction of OH with ΣANs produces either HNO_3 or NO_2 with a 6–30% yield. Calculations of NO fluxes constrained by the NO_2 observations and the inferred OH indicate that NO_x fluxes are downward into the canopy because of the substantial conversion of NO_x to HNO_3 and ΣPNs in the canopy. Even so, we derive that NO_x emission fluxes of ∼15 ng(N) m^{-2} s^{-1} at midday during summer are required to balance the NO_x and NO_y flux budgets. These fluxes are partly explained by estimates of soil emissions (estimated to be between 3 and 6 ng(N) m^{-2} s^{-1}). One possibility for the remainder of the NO_x source is large HONO emissions. Alternatively, the 15 ng(N) m^{-2} s^{-1} emission estimate may be too large, and the budget balanced if the deposition of HNO_3 and ΣPNs is slower than we estimate, if there are large errors in either our understanding of peroxy radical chemistry, or our assumptions that the budget is required to balance because the fluxes do not obey similarity theory.

Correspondence to: R. C. Cohen
(rccohen@berkeley.edu)

1 Introduction

Forests and other ecosystems constantly interact with the atmosphere, both emitting and removing chemicals including long-lived greenhouse gases (CO_2, N_2O, CH_4) as well as more reactive carbon compounds and nitrogen oxides. Natural terrestrial systems release 1150 Tg C/yr of volatile organic compounds (VOC) (Guenther et al., 1995) and 27 Tg/yr of N compounds (12, 9 and 6 Tg/yr of NO_x, NH_3 and N_2O respectively) (Schlessinger, 1997). With few exceptions, these VOC and nitrogen compounds have been thought to be emitted from leaves and soils and then transported out of the ecosystem canopy and into the boundary layer above on time scales of minutes, with oxidation occurring throughout the boundary layer. Effects associated with these large scale oxidation processes that have been of particular recent interest include the effects of biogenic isoprene mixing with anthropogenic NO_x on surface ozone (e.g. Fiore et

al., 2005), the role of biogenic VOC on secondary organic aerosol (e.g. Larsen et al., 2001; Kanakidou et al., 2005), the effects of some of the longer-lived VOC such as acetone on the greenhouse forcing due to their effects on the global distribution of tropospheric ozone (e.g. Collins et al., 2002), the contribution of nitrogen oxides to the natural background of ozone and secondary organic aerosol (e.g. Lelieveld et al., 2004; Kroll et al., 2005) and the contribution of nitrogen oxide deposition to soil nutrient levels (e.g. Takemoto et al., 2001).

Most of these prior studies either assume or calculate that within-canopy chemical reactions of nitrogen oxides or VOC arising from reaction with OH, O_3 or NO_3 are too slow to measurably affect fluxes. Important exceptions to this are the NO-O_3-NO_2, NH_3-$NH_4NO_{3(aerosol)}$-HNO_3 and sesquiterpene-O_3-product chemical systems. These systems can exhibit chemical flux divergence depending on the timescale of turbulence relative to the timescale of chemistry (Fitzjarrald and Lenschow, 1983; Brost et al., 1988; Kramm et al., 1995; Rummel et al., 2002; Nemitz et al., 2004). Prior models of reactive within-canopy chemistry and the associated trace gas fluxes typically calculate or assume OH in the range 5×10^4 to 1×10^6 molec cm^{-3} within the forest canopy, which is indeed low enough that there is little effect of OH within the canopy on fluxes (Kramm et al., 1991; Gao et al., 1993; Fuentes et al., 1996; Stroud et al., 2005; Forkel et al., 2006; Rinne et al., 2007). These concentrations are much lower than those in the boundary layer above the canopy because the shade of the canopy reduces sunlight that initiates OH production through photochemistry. Ozone reactions have also been thought of as too slow to be important to the flux of species other than NO and sesquiterpenes. NO_3 concentrations are thought to be too low to be important during daytime, but may be important to fluxes at night, although there is little theory or experiment available to evaluate this idea (Kramm et al., 1995).

There is growing evidence indicating that we should rethink these assumptions with respect to O_3 and OH. Observations have shown that there is rapid oxidation of sesquiterpenes and monoterpenes prior to their escape from the forest canopy, resulting in a significant upward flux of oxidized VOC (Goldstein et al., 2004; Holzinger et al., 2005b). O_3 has been assumed to be the primary oxidant in these processes (Kurpius and Goldstein, 2003; Goldstein et al., 2004; Holzinger et al., 2005b). Laboratory observations have shown that the reaction of ozone with unsaturated hydrocarbons (R1), including many terpenoids, has a product channel with significant (7–100%) yield of OH (Paulson and Orlando, 1996; Donahue et al., 1998; Kroll et al., 2001),

$$\mathrm{VOC} + \mathrm{O_3} \longrightarrow \mathrm{OH} + \mathrm{oxidized VOC} + \ldots \qquad \text{(R1)}$$

Thus there is a well defined chemical mechanism linking biogenic emissions of terpenoids and subsequent oxidation by O_3 to the production of OH. Reaction 1 has been invoked as a source of the OH observed in several field campaigns (Carslaw et al., 2001; Faloona et al., 2001; Tan et al., 2001). Goldstein et al. (2004) calculated that the terpenoid compounds emitted from a ponderosa pine forest at the University of California Blodgett Forest Research Station (UC-BFRS) would elevate OH levels in and above the canopy to 0.8–3.0×10^7 molec cm^{-3} based on the assumption of a high OH yield from R1. Prior to the nitrogen oxide flux observations described in this manuscript, these calculations by Goldstein et al. were the only observation-based suggestion that OH within a forest canopy might be higher than above. However, there are a number of OH observations indicating that emissions correlated with isoprene might be a significant source of OH, raising OH concentrations within and even high above forest canopies to well above those predicted by standard models (Faloona et al., 2001; Tan et al., 2001; Ren et al., 2006). Analysis of these observations provides hints of missing HO_x sources, while other studies have suggested that sinks are overestimated at low NO_x (Thornton et al., 2002). Consistent with the suggestion by Thornton et al. (2002), the recent observations of OH production in the reaction of oxygenated RO_2 with HO_2 (Hasson et al., 2004) may provide a partial explanation for the overestimate of HO_x sinks near forests.

Here we use observations of the fluxes of NO_2, ΣPNs, $\Sigma ANs_{(g+p)}$ and $HNO_{3(g+p)}$ to assess the mechanisms affecting canopy nitrogen oxide exchange and to characterize the photochemical environment within a forest canopy, with specific attention to within-canopy OH. We find that OH within the ponderosa pine canopy at the University of California-Blodgett Forest Research Station (UC-BFRS) is at least five times the concentration above the canopy and an order of magnitude more than the upper end of the range for OH (5×10^4–1×10^6 molec cm^{-3}) predicted in prior modeling studies of forest canopies (Gao et al., 1993; Stroud et al., 2005; Forkel et al., 2006). As we show in some detail here, within-canopy OH is a major factor affecting the fluxes of nitrogen oxides at this location. If the processes described here are important elsewhere, then a broad rethinking of the mechanisms of NO_y exchange above forests is necessary. In addition, high values of within-canopy OH will also affect O_3, VOC and secondary organic aerosol (SOA) chemistry; more quantitative analyses of the coupling of NO_x/VOC/O_3 and SOA will be needed before a complete understanding of forest-atmosphere interactions in the present and pre-industrial (with lower O_3 and lower NO_x) atmospheres can be achieved.

2 Field site and methods

The UC-BFRS flux site (120°53′42.9″N, 120°37′57.9″W, 1315 m elevation) is located in a managed ponderosa pine plantation near the UC-BFRS, and is owned by Sierra Pacific Industries. The vegetation is dominated by Pinus ponderosa L. that were planted in 1990. The median tree height

was 5.7 m, while the tallest trees in the canopy were 9 m and 80% of the trees were less than 7.3 m; leaf area index (LAI) ranged between 4 and 6 in the summer (Holzinger et al., 2005a). There are also individuals of Douglas fir, white fir, incense cedar and California black oak in the flux tower's footprint. The plantation understory is dominated by whitehorn (*Ceanothus cordulatus*) and manzanita (*Arcostaphylos spp.*) (Holzinger et al., 2005a). The site is located approximately 75 km downwind of the city of Sacramento. Due to the mountain-valley circulation, the site experiences daytime upslope flow and nighttime downslope flow with unusual regularity and a relatively narrow spread of wind direction (Murphy et al., 2006b). The site experiences a Mediterranean climate, with a hot, dry summer season and a cold, wet winter season. Previous studies have described the meteorology, chemical composition (CO, VOC, NO_y and O_3) and O_3 and CO_2 fluxes at this site (Bauer et al., 2000; Goldstein et al., 2000; Dillon et al., 2002; Day et al., 2003; Holzinger et al., 2005b; Murphy et al., 2006a; Murphy et al., 2006b; Murphy et al., 2006c). Note that this study took place one year later, and both the forest canopy and measurement height were approximately two meters higher, than the study described by Holzinger et al. (2005b).

We use thermal dissociation – laser induced fluorescence (TD-LIF) (Day et al., 2002) in an eddy covariance mode (Farmer et al., 2006) to measure the full annual cycle (June 2004–June 2005) of fluxes of NO_2, total peroxy and peroxy acyl nitrates (ΣPNs, $\Sigma R_iO_2NO_2$), total alkyl and multifunctional alkyl nitrates (ΣANs, ΣR_iONO_2), including aerosol phase ΣR_iONO_2, and total gas plus semi-volatile particle bound $HNO_{3(g+p)}$ (Bertram and Cohen, 2003) on a walk-up tower at a point 7 m (14.3 m above ground level, a.g.l.) above the UC-BFRS forest canopy (7.3 m a.g.l.). The semi-volatile aerosol component of the HNO_3 measurement is believed to be negligible at Blodgett Forest during the summer due to low ambient ammonia levels (Fischer and Littlejohn, 2006).

The TD-LIF instrument has two major subsystems: a heated inlet and an NO_2 detector. Air is pulled through the modestly heated fore-inlet where the temperature is kept high enough to ensure complete transmission of HNO_3 (Neuman et al., 1999), but low enough to prevent dissociation of peroxy nitrates (Farmer et al., 2006). The sample is then split into four separate heated quartz tubes for each of the four classes of reactive nitrogen oxide species ($HNO_{3(g+p)}$, $\Sigma ANs_{(g+p)}$, ΣPNs, NO_2). At the residence times characteristic of this experiment, these compounds dissociate to NO_2 and an accompanying radical at 550°C, 330°C, 180°C, or are present in the ambient air, respectively (Day et al., 2002). The mixing ratio of each class of NO_{yi} is determined as the difference in NO_2 detected in adjacent-temperature channels. For example, ΣPNs are the difference in NO_2 observed between the 180°C and ambient temperature channels. Both gaseous and semi-volatile aerosol components of HNO_3 and ΣANs are dissociated to NO_2 in the 550°C and 330°C channels, respectively. Salts such as $NaNO_3$ are not detected. The temporal response of the inlet is rapid enough that it has little effect on the flux measurements (Farmer et al., 2006).

The sample proceeds from the inlet in PFA tubing down the tower to the laser-based detection system housed in a temperature-controlled trailer at the foot of the tower. NO_2 is detected by LIF using a narrow band etalon-tuned 585 nm dye laser pumped by a 532 nm diode-pumped, frequency-doubled, pulsed Nd:YAG laser (Spectra Physics) (Thornton et al., 2000). The dye laser is tuned to a specific rovibronic feature of NO_2, and is alternated between this feature and a weaker continuum absorption to test for interferences and maintain a line-locking algorithm. The laser is focused through a series of four multi-pass White cells, one for each channel. The resulting red-shifted fluorescent photons are imaged onto a photomultiplier tube (Hamamatsu H7421-50) and collected using time-gated counting after a delay that eliminates prompt scattering. The NO_2 mixing ratio is directly proportional to the fluorescence signal, and is detected at 5 Hz with a sensitivity that varied in the range of 24–64 pptv in 0.2 s (S/N=2) during the course of the year-long experiment. As described in detail in Farmer et al. (2006), the flux is calculated every half-hour as the covariance between observed mixing ratios and vertical wind speed, measured by a sonic anemometer (Campbell Scientific CSAT3 3-D Sonic Anemometer). Instrument noise affects fluxes systematically by <15%, while spectral attenuation and sensor separation contribute to under-estimation of fluxes by <7% and <20%, respectively (Farmer et al., 2006). Temperature was derived from the sonic anemometer and used to calculate sensible heat fluxes, or, more correctly, buoyancy fluxes.

Concentration measurements of NO_2, ΣPNs and HNO_3 by TD-LIF have been compared in the field to observations by independent techniques at the surface and by aircraft. In general, there has been average agreement to better than 15% with differences limited by precision of the measurements. In some cases, mean differences of up to 30% were observed and identified as due to issues in design of one of the variations we have developed for the TD-LIF inlet. The inlet used in the experiments described here does not suffer from this design error and these other comparison experiments suggest it is not expected to exhibit any interferences due to sampling or unexpected secondary chemistry within the heated regions (Thornton et al., 2003; Bertram, 2006; Wooldridge et al., in preparation).

3 Results

During the winter (January–March) when conditions were cold, snowy and wet, we observed upward fluxes (emission) of NO_2, and downward fluxes (deposition) of ΣPNs, $\Sigma ANs_{(g+p)}$, $HNO_{3(g+p)}$, and of the sum of NO_2+ΣPNs+$\Sigma ANs_{(g+p)}$+$HNO_{3(g+p)}$ (Farmer et al., 2006). These results are qualitatively what were expected from these measurements, namely an upward flux of NO_2 resulting from

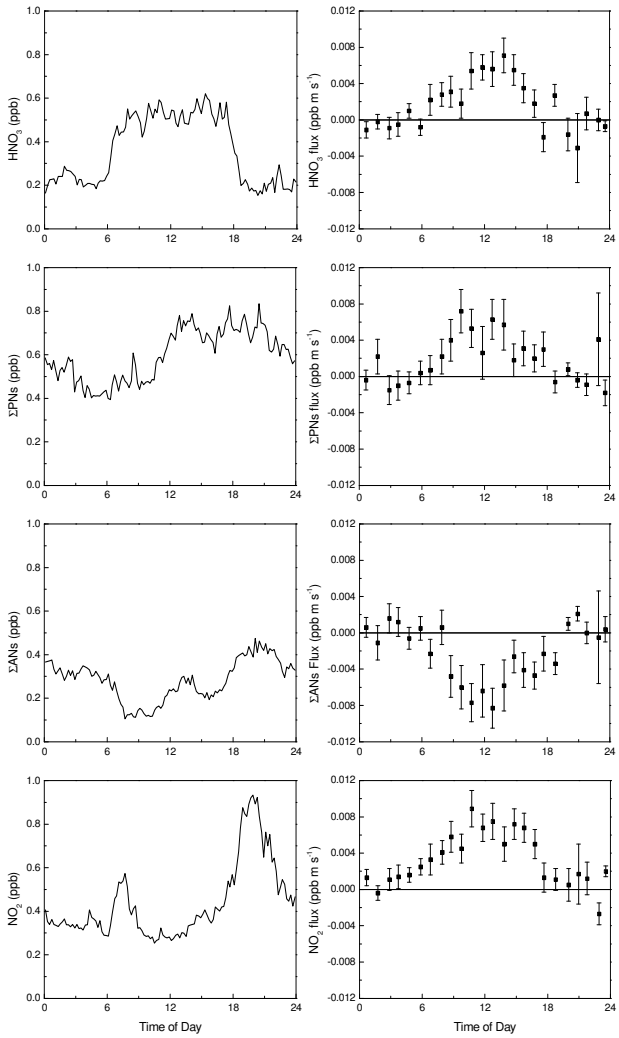

Fig. 1. Average August 2005 UC-BFRS mixing ratios (left column, ppb) of NO_2, total peroxy and peroxy acyl nitrates (ΣPNs), total alkyl and multifunctional alkyl nitrates (ΣANs) and HNO_3. Net fluxes (right, ppt m s^{-1}) of HNO_3, ΣPNs and NO_2 are upward out of the canopy in the daytime; ΣANs are downward into the canopy. Nighttime fluxes are near zero. Fluxes are monthly averages, and error bars represent the variance of fluxes over the entire month.

conversion of NO to NO_2 within the canopy and downward fluxes of the higher oxides. Deposition of HNO_3 has been widely reported (e.g. Lefer et al., 1999; Sievering et al., 2001; Tarnay et al., 2001; Pryor et al., 2002), with the few measurements of upward fluxes generally attributed to flux divergence due to interconversion between gas and particle phase HNO_3 (Brost et al., 1988; Huebert et al., 1988; Neftel et al., 1996; Van Oss et al., 1998; Pryor et al., 2002; Nemitz et al., 2004). Note that since our measurement is the sum of both phases of HNO_3, this mechanism is only relevant to interpretation of our measurements to the extent that gas and particle phase HNO_3 have different deposition velocities. Further, the low NH_3 concentrations (0.5 ppb< observed <1.5 ppb; $K_p \gg [NH_3][HNO_3]$) at the site imply that, at least during the summer, there is no semi-volatile aerosol that could affect the HNO_3 fluxes (Fischer and Littlejohn, 2006). To our knowledge, there are no prior measurements of alkyl nitrate fluxes. ΣANs are a mixture of a wide range of compounds (O'Brien et al., 1995; Kastler et al., 2000; Day et al., 2003; Rosen et al., 2004; Cleary et al., 2005), many of which are hydroxyalkyl nitrates that are expected to have high deposition velocities because the hydroxyl group enhances their solubility in water (Shepson et al., 1996; Treves and Rudich, 2003). Peroxyacetyl nitrate (PAN) deposition has been observed over various grassland and forest ecosystems (Shepson et al., 1992; Schrimpf et al., 1996; Turnipseed et al., 2006), though upward PAN fluxes have been observed on hot days in the presence of precursors (Doskey et al., 2004). Upward NO_2 fluxes have been observed previously, and are attributed to NO reactions with O_3 and decreases in the NO_2 photolysis rate within forest canopies relative to above them (Gao et al., 1993; Horii et al., 2004).

During summer (June–August) when conditions were hot and dry, we observed emission of the individual species NO_2, ΣPNs and $HNO_{3(g+p)}$, deposition of ΣANs, and emission of the sum $\Sigma(NO_2+PNs+ANs+HNO_{3(g+p)})$ (Fig. 1 shows observations averaged by time of day for August 2004). These results were typical of other summer months. As in winter, the NO_2 flux is expected to result from conversion of NO to NO_2 within the forest canopy. During summer, soil emissions of NO are also expected to contribute to the canopy scale NO_x flux, as has been observed at a number of other sites (e.g. Rummel et al., 2002). In contrast, the measurements of $HNO_{3(g+p)}$ emission from the canopy are unexpected and contrary to the commonly accepted notion that HNO_3 is produced at a roughly constant rate throughout the boundary layer and removed at the surface by either dry deposition (as gas or particle) or rainfall. ΣPN emission is also surprising as PAN has generally been observed to deposit (e.g. Turnipseed et al., 2006). Extensive tests of the instrumentation and observing strategy confirm the measurements are accurate to within 15%, and that the upward fluxes are not an artifact of either our procedures, or of the topography of the UC-BFRS site (Farmer et al., 2006).

4 Winter observations

The winter observations provide no indication that unusual processes need to be invoked. Accordingly, we assume a standard model to interpret the fluxes in winter. The mechanisms controlling fluxes during the winter, and a more detailed comparison of wintertime measurements to observations at other sites will be presented in a separate manuscript. Here we focus on winter primarily as a point of reference for evaluating the chemical mechanisms affecting summertime NO_{yi} fluxes.

We estimate the gradients in NO_x, ΣPNs, ΣANs and HNO_3 from the chemical fluxes using three methods: 1) assuming similarity to CO_2 fluxes and gradients, 2) using Monin-Obukhov similarity theory, as described in detail by Fuentes et al. (1996) and 3.) using the surface renewal model described by Holzinger et al. (2005b). We note that the flux measurements are made at 14.3 m, approximately twice the canopy height, and that some breakdown of similarity theory is expected. The comparison of these different calculations provides some indication of the potential magnitude of this breakdown and its effects on our conclusions.

Vertical profiles of oxidized VOC at UC-BFRS show maxima indicative of significant oxidation between 5 and 9 m (Holzinger et al., 2005b), and we choose the mid-point of this range just above the canopy, 7m, as a reference height. Typical NO_2, ΣPN, $\Sigma AN_{(g+p)}$ and $HNO_{3(g+p)}$ noontime winter fluxes are +1.4, –0.89, –2.46 and –1.5 ppt m s^{-1} (1 ppt m $s^{-1} \approx 1.47\times10^5$ μmol m^{-2} $h^{-1} \approx 0.5726$ ng(N) m^{-2} s^{-1}) and the corresponding concentrations above the canopy are 0.223, 0.205, 0.098, and 0.050 ppb, respectively. We derive NO_{yi} gradients from the assumption that the same eddies carry the fluxes of two scalars, (F_{c1}) and fluxes (F_{c2}). In this approximation, known as the modified Bowen ratio, it is assumed that the ratio of any flux to the gradient of that species or scalar are equal (Meyers et al., 1989):

$$\frac{F_{c1}}{\Delta C_1} = \frac{F_{c2}}{\Delta C_2} \tag{1}$$

where ΔC_1 and ΔC_2 are the mixing ratio gradients, corresponding to the fluxes F_{c1} and F_{c2} respectively. Rearranging Equation 1 to solve for the mixing ratio gradient of a given compound gives, in terms of the other three quantities:

$$\Delta C_2 = F_{c2} \times (\Delta C_1 / F_{c1}) \tag{2}$$

Observations of the fluxes and gradients of both CO_2 and water are available to test the accuracy of Eq. 2 (Goldstein et al., 2000). During the winter, we find that the equation is consistent with the measurements within a factor of 2 and we estimate that the uncertainty as applied to the NO_{yi} species is at least that large. Typical observed winter CO_2 fluxes were –24.8 mmol m^{-2} hr^{-1} (–0.186 ppm m s^{-1}) and typical gradients are 1.06 ppm. Using the observed CO_2 flux gradient and extrapolating the gradient from the measured heights of 1.2, 3.0, 4.9, 6.8 and 10.5 m to our measurement height at 14.3 m, we calculate the gradients of NO_2, ΣPNs, ΣANs and HNO_3 between the measurement height of 14.3 m and 7 m above the ground to be +8.0, –5.1, –14, and –8.6 ppt, respectively.

As a second approach, we use Monin-Obukhov theory to calculate the flux-gradients. In this approach, equations relating the concentration gradients to the fluxes are then:

$$\Delta C = C_2 - C_1 = \frac{F_C}{\kappa u_*}\left(\ln\left(\frac{z_2 - d}{z_1 - d}\right) + \Psi c_1 - \Psi c_2\right) \tag{3}$$

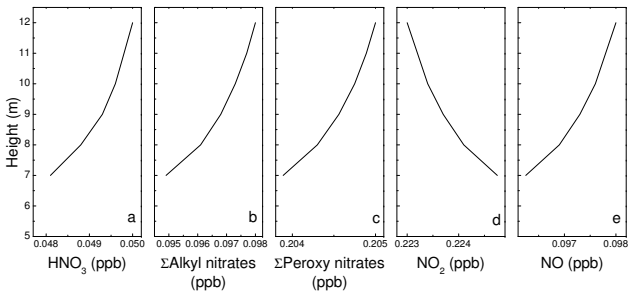

Fig. 2. Calculations using the CO_2 similarity theory for the midday winter gradients in HNO_3, ΣANs, ΣPNs, NO_2 and NO required to produce observed fluxes. NO_x is assumed to be constant (0.321 ppb) through the entire vertical profile in winter, with zero net flux.

where z is the height a.g.l., κ is the von Karman constant (0.4), L is the Monin-Obukhov length, u_* is the friction velocity, d is the zero plane displacement height, and Ψ_c is a stability parameter,

$$\Psi_c = 2\ln\left(\frac{1 + x^2}{2}\right) \tag{4}$$

where

$$x = \left(1 - \frac{16z}{L}\right)^{1/4} \tag{5}$$

The NO_{yi} gradients calculated by the modified Bowen ratio with CO_2 as the reference compound are 10–20% larger than those calculated using the Monin-Obukhov theory (Table 1).

Our third approach is to calculate flux-gradient relationships using the surface-renewal method, as described by Holzinger at al. (2005b). In this method, the production rate (P_c), or flux, of a species is determined by the amount in excess (EA_c) over background ($[c]_B$) produced in a given mixing time (t_{mix}),

$$P_c = \frac{EA_c}{t_{\mathrm{mix}}} \tag{6}$$

$$EA_c = \int_0^h [c]dz - h[c]_B \tag{7}$$

Assuming similarity in the vertical exchange, an unknown excess can then be derived from the ratio of two observed fluxes and one known excess:

$$P_{c1} = \frac{EA_{c1}}{EA_{c2}} P_{c2} \tag{8}$$

We integrated the observed CO_2 gradients to calculate an excess of 22.9 ppm·m between our measurement height (14.3 m) and ground level. This excess concentration corresponds to the observed –0.186 ppm m s^{-1} CO_2 flux. Substituting into Eq. 8 results in the –1.5 ppt m s^{-1} HNO_3 flux corresponding to a –184.5 ppt·m excess over background. For

Table 1. Winter noon-time concentrations and fluxes of NO, NO_2, ΣPNs, ΣANs and HNO_3 at 14.3 and 7 m a.g.l.: Fluxes (14.3 m height, ppt m s^{-1}) and mixing ratios (ppb) at 14.3 m and 7 m a.g.l. were observed, estimated from previous measurements (†) or modelled by steady-state approximations (§) and the flux gradient approach (‡) as described in this paper. NO_y (∞) is calculated as the sum of NO, NO_2, ΣPNs, ΣANs and HNO_3. Within-canopy mixing ratios are calculated using Monin-Obukhov (MO), modified Bowen ratio/CO_2 similarity (BR) and surface renewal (SR) theories. Excess mixing ratio below the measurement height was calculated by the surface renewal approach.

Species	Flux (ppt m s^{-1})	14.3 m mixing ratio (ppb)	Excess (ppt·m, SR)	7 m mixing ratio (ppb, SR)	7 m mixing ratio (ppb, MO)	7 m mixing ratio (ppb, BR)
NO	–1.4‡	0.098†	–172	0.090§	0.091§	0.090§
NO_2	+1.4	0.223	+172	0.231‡	0.230‡	0.231‡
ΣPNs	–0.9	0.205	–111	0.200‡	0.200‡	0.200‡
ΣANs	–2.5	0.098	–308	0.084‡	0.085‡	0.084‡
HNO_3	–1.5	0.050	–185	0.041‡	0.042‡	0.041‡
ΣNO_{yi}	–4.9∞	0.674∞		0.647∞	0.648	0.647

the sake of comparison, we assume that the CO_2 and NO_{yi} profiles have the same shape, and that the ratio of the integral between 7 and 14.3 m to the integral of the total column is consistent for different chemical species. In this way, we arrive at an estimate of the HNO_3 gradient between 7 and 14.3 m of 9 ppt.

We calculate the exchange velocities (V_{ex}) from the observed flux (F) and mixing ratio (C),

$$V_{ex} = \frac{F}{C} \tag{9}$$

A negative V_{ex} indicates a downward, deposition flux, while a positive V_{ex} represents an upward, emission flux; the deposition velocity, V_{dep}, is $-V_{ex}$. The median noon-time winter V_{ex} were –2.5, –2.0 and –0.8 cm s^{-1} for $HNO_{3(g+p)}$, $\Sigma ANs_{(g+p)}$ and ΣPNs respectively at UC-BFRS (Farmer et al., 2006). These exchange velocities are in the range of previous observations for HNO_3 (e.g. Sievering et al., 2001; Tarnay et al., 2001; Pryor et al., 2002; Pryor and Klemm, 2004) and PAN (Shepson et al., 1992; Schrimpf et al., 1996; Turnipseed et al., 2006). Horii et al. (2005) used NO_y flux measurements at Harvard Forest to infer a –3 cm s^{-1} exchange velocity for a "missing NO_y flux" component that was not due to HNO_3 or PAN, and was identified as most likely due to isoprene-derived hydroxyalkyl nitrates. Their value of 3 cm s^{-1} for the deposition velocity of this ΣAN-like fraction of NO_y is similar to the 2 cm s^{-1} that we derive for ΣANs directly from measurements.

The V_{ex} for NO_2 is +0.63 cm s^{-1} in the winter at midday. Sources of NO_x in the forest canopy during winter are expected to be very small, and, to a first approximation, we assume that the observed flux is entirely driven by conversion of NO to NO_2 below the canopy and that NO_x is therefore constant throughout the canopy during winter. Analysis of the NO to NO_2 ratio is simplified if we can assume steady-state which requires residence times longer than 100 s. The residence time can be calculated by Eq. 9 (Martens et al., 2004),

$$\tau = h_c \times R_t \tag{10}$$

where τ is the residence time, h_c is the height, and R_t is the total aerodynamic resistance for a molecule passing through the canopy atmosphere, or the sum of aerodynamic and boundary layer resistances. For HNO_3, R_t can be approximated as $1/V_{\mathrm{dep,\,HNO_3}}$, and the residence time for a molecule below the 14.3 m sensor height is 570 s in the winter. Alternatively, the estimate can be made using the surface renewal model (Eq. 6). For winter that model suggests a residence time of 123 s. The accuracy of residence time estimates is not well-understood and reasonable arguments for both values can be made. In the context of our analysis, the "residence time" refers to the average amount of time a molecule spends in the forest canopy – between the ground and our sensor – and is able to participate in chemical reactions. Given the uncertainty, we discuss residence times derived from both approaches throughout the manuscript. Both estimates are long enough that NO and NO_2 should reach steady state prior to being sampled as a result of the reactions:

$$NO_2 + h\upsilon(+O_2) \rightarrow NO(+O_3) \tag{R2}$$

$$NO + O_3 \rightarrow NO_2 + O_2 \tag{R3}$$

$$NO + RO_2 \rightarrow NO_2 + RO \tag{R4}$$

$$NO + HO_2 \rightarrow NO_2 + OH \tag{R5}$$

NO and NO_2 are therefore related by the equation:

$$\frac{NO}{NO_2} = \frac{J_{NO_2}}{k_3\,[O_3] + k_4\,[RO_2] + k_5\,[HO_2]} \tag{11}$$

where J_{NO_2} is the NO_2 photolysis rate and k_3–k_5 are the rate constants for reactions 3 to 5. J_{NO_2} at the measurement height (14.3 m) was calculated from the Tropospheric Ultraviolet and Visible Radiation (TUV) model to be 0.0074 s^{-1}

(Madronich and Flocke, 1998). Previous observations of the above-canopy NO to NO_2 ratio (Day, 2003) and the observed 0.223 ppb NO_2 imply 0.098 ppb NO at 14.3 m. Winter NO concentrations at other heights can then be estimated using any of the flux gradient relationships described above for NO_2 and our assumption of zero NO_x flux. For simplicity, we use the modified Bowen ratio with CO_2 as the reference compound (values from the other methods are shown in Table 1). The –1.4 ppt m s^{-1} NO flux corresponds to an 8 ppt gradient, and thus 0.090 ppb NO at 7 m a.g.l. Observed O_3 fluxes during winter are too small to produce a gradient that would affect the ratio of NO to NO_2; during winter the RO_2 and HO_2 terms are smaller than the O_3 term (<10%; $[HO_2+RO_2]=1.6\times10^8$ molec cm^{-3}), and thus will also contribute little to the NO_x gradient. Substituting the measured and inferred NO and NO_2 concentrations at the different heights into Equation 9, we can derive the attenuation of photolysis rates at the different heights. Because of the open canopy structure, we expect very little attenuation of the photolysis rate, and, consistent with that expectation, we calculate the photolysis rates at 7m agl to be 89% of the measurement height J_{NO_2}.

The net winter ΣNO_{yi} fluxes are calculated as the sum of the four observed fluxes (NO_2, ΣPNs, $\Sigma ANs_{(g+p)}$ and $HNO_{3(g+p)}$) and the inferred NO flux; the noon-time ΣNO_{yi} flux is –4.9 ppt m s^{-1} at a total NO_{yi} concentration of 0.67 ppb, a value that is in the range of previous observations (Munger et al., 1996). Thus the net V_{ex} for ΣNO_{yi} is –0.73 cm s^{-1}.

5 Summer observations

We have considered numerous possible explanations for our observations of upward fluxes of $HNO_{3(g+p)}$ and ΣPNs during summer. The only hypothesis we have been able to develop that is consistent with all of the available data, including previous observations at this and nearby sites (e.g. Murphy et al., 2006a), is that our sensor is located above the peak ΣPN and HNO_3 concentrations because there is a chemical source of these species associated with emissions from the forest canopy. In what follows, we develop a model showing that this hypothesis is plausible. Some aspects of this model are poorly constrained and additional laboratory and field observations will be needed to test whether some of the predictions of our model are correct.

As we did for winter, we estimate the summer gradients in NO, NO_2, ΣPNs, $\Sigma ANs_{(g+p)}$ and $HNO_{3(g+p)}$ using the flux-gradient approach, the Monin-Obukhov calculation and the surface renewal models described above (Eqs. 1 to 8). Typical summer CO_2 gradients between 7 and 14.3 m a.g.l. are 4.59 ppm at noon, with a corresponding observed flux of –25.002 mmol m^{-2} hr^{-1} (–0.1976 ppm m s^{-1}) and an excess concentration of 14.2 ppm·m. Corresponding summer H_2O gradients, fluxes and excess concentrations

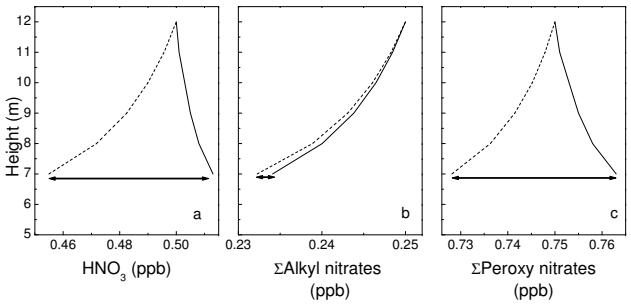

Fig. 3. *Panels a-c:* Calculations using the CO_2 similarity theory for the midday summer gradients in ΣANs, HNO_3, and ΣPNs required to produce observed fluxes (solid) and calculations of the deposition fluxes (dashed). Horizontal arrows represent the implied within canopy chemical source of HNO_3, ΣANs and ΣPNs.

are –0.1969 ppth (parts per thousand), 17.553 mol m^{-2} hr^{-1} (0.1387 ppth m s^{-1}), and 9.9864 ppth· m. The modified Bowen ratio for CO_2 and H_2O (Eq. 1) agrees to within 12%. The closer correspondence for these calculations in the summer than in the winter is consistent with the presence of much more vigorous turbulence in the summer. During summer, CO_2 gradients calculated using the Monin-Obukhov calculations are about three times larger than calculated by the modified Bowen ratio, indicating that even with this more vigorous mixing, turbulent dynamics are not in a far field limit. The surface renewal model applied to CO_2 and water gives agreement with the excess calculated water using the water flux and CO_2 flux and excess as inputs to within 15%. Holzinger et al. (2005b) report accuracy of the surface renewal approach to within 30%. Since CO_2, water and NO_{yi} are all expected to have sources and sinks at similar heights, and the simpler modified Bowen ratio accurately represents the relationship of CO_2 and water fluxes and gradients, we use this calculation as the point of reference in the remainder of the text. Calculations using the other two models are included to give some indication of the range of conclusions that would be consistent with the different models.

Typical NO_2, ΣPN, $\Sigma AN_{(g+p)}$ and $HNO_{3(g+p)}$ noontime summer fluxes are 7, 5, –6 and 5 ppt m s^{-1}, and the corresponding above-canopy concentrations are 0.30, 0.75, 0.25, and 0.50, respectively (Table 2). Using these numbers, CO_2 as a reference compound and Eq. 2, we calculate the gradients of NO_2, ΣPNs, $\Sigma ANs_{(g+p)}$ and $HNO_{3(g+p)}$ between the measurement height of 14.3 m and 7 m above the ground to be 11, 7.9, –9.5, and 7.9 ppt, respectively (Table 2). The calculated NO_{yi} gradients are shown as solid lines in Figs. 3 and 4, and are used in the calculations presented below. Some of the conclusions presented below also depend on the residence times. Using Eqs. 6 and 10, we derive residence times of 420 and 72 s during the summer, compared to the 100 second ramp time observed by Holzinger et al. (2005b).

Table 2. Summer noon-time concentrations and fluxes of NO, NO_2, ΣPNs, ΣANs and HNO_3. Fluxes (14.3 m height, ppt m s^{-1}) and mixing ratios (ppb) at 14.3 m and 7 m a.g.l. were observed, estimated from previous measurements (†) or modelled by steady-state approximations (§) and the flux gradient approach (‡) as described in this paper. The predicted contributions to within-canopy mixing ratio (7 m) from deposition were determined from observed winter V_{dep} scaled by turbulence (*), while contributions from $NO_x \leftrightarrow NO_z$ chemistry were assumed responsible for the differences between observed and predicted fluxes (^). NO_y (∞) is calculated as the sum of NO, NO_2, ΣPNs, ΣANs and HNO_3. Within-canopy mixing ratios are calculated using Monin-Obukhov (MO), modified Bowen ratio/CO_2 similarity (BR) and surface renewal (SR) theories; gradients that are due to separate effects of deposition or chemistry are calculated using the CO_2 flux-gradient. Excess mixing ratio below the measurement height was calculated by the surface renewal approach.

Species	14.3 m mixing ratio (ppb)	Excess (ppt·m, SR)	7 m mixing ratio (ppb) (SR)	7 m mixing ratio (ppb) (MO)	7 m mixing ratio (ppb) (BR)	Flux (ppt m s^{-1})	Gradient due to deposition (ppt)	Gradient due to chemical conversion of NO_x to NO_z (ppt)
NO	0.054†	–468	0.019§	0.012§	0.019§	–16‡	–	–4§
NO_2	0.30	503	0.311‡	0.329‡	0.311‡	7	–	–54§
ΣPNs	0.75	360	0.758‡	0.771‡	0.758‡	5	–13*	21^
ΣANs	0.25	–431	0.240‡	0.225‡	0.241‡	–6	–11*	2^
HNO_3	0.50	360	0.508‡	0.521‡	0.508‡	5	–27*	35^
ΣNO_{yi}	1.854∞		1.885∞	1.858∞	1.837∞	–5∞	–51∞	0∞

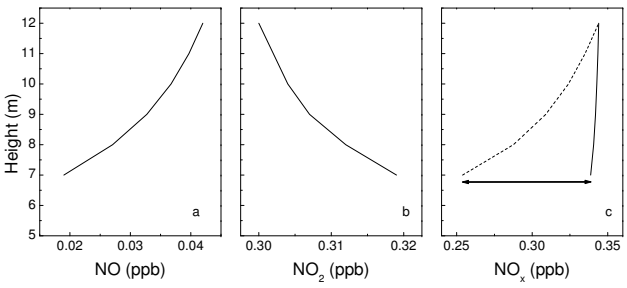

Fig. 4. The gradients in NO, NO_2 and NO_x (≡ NO + NO_2) derived from the observations (see text for details). The solid line represents the NO_x profile calculated as the sum of NO and NO_2 profiles. The dashed-line represents the NO_x gradient that we predict would be a result of within-canopy chemistry if there were no emission of NO_x. The difference between the dashed and solid lines shown with the double-headed arrow represents net ecosystem NO_x emission.

5.1 HNO_3

For a well-mixed system in steady-state, surface deposition of HNO_3 is balanced by chemical production of HNO_3. Daytime photochemical production of HNO_3 occurs primarily by the reaction of OH with NO_2,

$$OH + NO_2 \rightarrow HNO_3 \quad \text{(R6)}$$

The daily variation of the $HNO_{3(g+p)}$ mixing ratio at UC-BFRS follows that of the solar irradiance, with little lag, confirming a strong daytime photochemical source in near steady-state with sinks, as has been reported for other sites (e.g. Lefer et al., 1999; Brown et al., 2004). Equating HNO_3 production by reaction with OH with loss to noon-time deposition, OH can be estimated as:

$$OH = \frac{V_{dep} \times HNO_3}{k_{OH+NO_2} \times NO_2 \times h} \quad (12)$$

where k_{OH+NO_2} is the rate constant for R6 and h is the boundary layer height. We observe noontime NO_2 of 0.3 ppb and $HNO_{3(g+p)}$ of 0.5 ppb, and use k_{OH+NO_2} (25°C, 868 mbar) of 9.85×10^{-12} molec^{-1} cm^3 s^{-1} (Sander et al., 2006). We scale the deposition velocity of 2.5 cm s^{-1} obtained from the noon-time winter data by the ratio of the average noon-time friction velocity to derive a summer noon-time V_{dep} of 3.4 cm s^{-1}, and assume a 1000 m boundary layer height. Inserting these quantities into Eq. 12, we derive a boundary layer average OH of 5.7×10^6 molec cm^{-3}. Although the heights are not well known, several factors act to suppress boundary layer growth in the foothills and Central Valley, including the daytime upslope advection, return flows moving to the west aloft, and large-scale westerlies; a lower boundary layer height would not be surprising (Seaman et al., 1995; Kossmann et al., 1998; Carroll and Dixon, 2002; Dillon et al., 2002). Another uncertainty in this calculation arises because at least some of the HNO_3 is transported from upwind where NO_x concentrations are much higher (Murphy et al., 2006a) and thus observed HNO_3 is likely larger than the steady-state value, causing an over-estimate of OH.

The 3.4 cm s^{-1} deposition velocity, calculated by scaling the wintertime $V_{dep,}$ implies a HNO_3 deposition flux of –17 ppt m s^{-1}, and, in the absence of chemical production, would result in a decrease in HNO_3 at 7 m of 26.9 ppt relative to 14.3 m, shown as the dashed line in Fig. 3. The positive gradient of 7.9 ppt that we calculate from the observed fluxes implies a chemical production of 34.8 ppt during the residence time of air between the ground and the sensor; this is shown as the black arrow in Fig. 3.

We assume the only source of HNO_3 is the reaction of OH with NO_2. The product of OH and residence time required to produce 34.8 ppt of HNO_3 from the 311 ppt of NO_2 we calculate to be present at 7 m is 1.1×10^7 molec OH cm^{-3} s, which corresponds to a range of approximately 2.7 to 16×10^7 for

the 72 to 420 s range in estimated residence times. The surface renewal approach provides an alternate route to calculation of OH. Using the excess of 360 ppt·m HNO_3 over background and assuming an identical profile to CO_2, we find an excess concentration of 8 ppt at 7 m. The product of OH and residence time required to produce that 8 ppt excess from the approximately 311 ppt NO_2 calculated to be between the surface and 7 m is 1.1×10^{10} molec OH cm^{-3} s (product of OH and residence time). This corresponds to a range of OH of 2.7 to 16×10^7 molec OH cm^{-3} for the 72 to 420 s range of residence times. The low end of the ranges in these modified Bowen ratio, Monin-Obukhov theory and surface renewal calculations are about five times larger than the 5.7×10^6 molec OH cm^{-3} we calculate as the boundary layer average, and the high end of this range is almost thirty times larger than the boundary layer average. If these OH estimates – or, more accurately, these estimates of the product of OH and canopy residence time – are correct, then they will also be consistent with the gradients we infer for ΣANs, ΣPNs and NO_2 and NO_x.

5.2 ΣANs

As for HNO_3, the ΣAN gradient is due to the balance of deposition and within-canopy chemistry. Scaling the wintertime V_{dep} of 2.0 cm s^{-1} by the friction velocity results in a 2.7 cm s^{-1} estimate of the summer V_{dep} and a deposition flux of –6.7 ppt m s^{-1}. Using this value and 0.25 ppb ΣANs in the CO_2 similarity approach results in an estimate of the ΣAN gradient at 7 m of –10.6 ppt, compared to –9.5 ppt calculated from observed fluxes. Thus net chemical production of ΣANs must be small, of order 1 ppt. This is surprising as the high OH we infer must be associated with rapid chemical production of ΣANs.

The chemical source of ΣANs is the minor channel in the reaction of RO_2 with NO (R4):

$$RO_2 + NO \rightarrow RONO_2 \quad \text{(R7)}$$

The branching ratios for R4b for individual compounds that are important to the VOC reactivity at UC-BFRS (Lamanna and Goldstein, 1999) vary widely, but are typically in the range of 1–20% (Atkinson et al., 1982; O'Brien et al., 1998).

Chemical production of ΣANs is given by:

$$P_{ANs} = \Sigma\alpha_{4i}k_{4i}[R_iO_2][NO] = \alpha_{eff}k_{eff}[RO_2][NO] \quad (13)$$

where $\alpha_4 = k_{4b}/(k_{4a}+k_{4b})$. In our previous studies in urban plumes, we found that the effective branching ratio for a mix of hydrocarbons, α_{eff}, was calculated to be 4%, and that a branching ratio of 4–6% would be consistent with the observed correlation of O_3 and ΣANs (Rosen et al., 2004; Cleary et al., 2005). We estimate ΣAN production by solving for HO_2, RO_2 and NO in steady state based on the kinetics of Reactions 3 to 9:

$$RO_2 + RO_2 \rightarrow \text{products} \quad \text{(R8)}$$

$$RO_2 + HO_2 \rightarrow \text{products} \quad \text{(R9)}$$

$$HO_2 + HO_2 \rightarrow \text{products} \quad \text{(R10)}$$

We use the 7 m OH derived from the HNO_3 fluxes and the OH loss rate to reaction with VOC at UC-BFRS of 8.4 s^{-1}. We arrive at this estimate by starting with the observations of Lamanna and Goldstein (1999), who determined a mean summer OH loss rate of 5.6 s^{-1} from C_2-C_{10} VOC measurements. These measurements did not include the very reactive biogenic VOC reported by Holzinger et al. (2005b) or H_2CO and thus are an underestimate. We use the results from Di Carlo et al. (2004), who showed in a different ecosystem that typical VOC measurements underestimate OH loss rates by as much as a factor of 1.5. We scale the Lamanna and Goldstein (1999) loss rate by this factor. This OH loss rate gives an RO_2 production rate of approximately 2.4×10^8 molec cm^{-3} s^{-1}. The other constants required in our calculation of ΣAN production are α_{eff}=0.04, NO_2=0.311 ppb, and $J_{NO_2,\text{in-canopy}}$=0.0085 s^{-1}. We use the low end of previous observations of α_{eff} because of the large contribution of low-yield species such as isoprene, CH_4 and 2-methyl-3-buten-2-ol (MBO) to the measured reactivity at this site, and our estimate that formaldehyde (H_2CO), which has a zero nitrate yield, is also an important component of the reactivity. The photolysis rate is estimated as 89% of the above-canopy J_{NO_2} based on the inference from the winter measurements. A typical summer noon-time above-canopy photolysis rate is 0.0095 s^{-1}, calculated from the TUV model (Madronich and Flocke, 1998). With these constraints, we calculate 1.2×10^{10} and 2.5×10^9 molec cm^{-3} of RO_2 and HO_2, respectively, at 7 m a.g.l. For comparison, the RO_2 and HO_2 we calculate at the measurement height are 2.7×10^9 and 1.7×10^9 molec cm^{-3}, respectively. Note that RO_2 is calculated to be 5 times larger than HO_2 as a result of the very low NO of 0.019 ppb, and that these high RO_2 and HO_2 concentrations result in the unusual situation of RO_2 and HO_2 being the dominant terms in the denominator of Equation 11. We calculate an in-canopy NO to NO_2 ratio of 0.06, compared to the 0.18 ratio observed above the Blodgett Forest canopy (Day, 2003). Inserting these numbers into Eq. 13, we calculate that 28 ppt ANs are produced chemically in the 400 s residence time, and that the net gradient produced by the combined effects of deposition and chemical production would be +17 ppt. If, as is the case for HNO_3, there were no other OH-driven processes acting on the time scale of canopy exchange, this is the gradient we would expect to observe, which would result in an upward flux for a 400 s residence time, in contrast to the observed deposition. A 70 s residence time and the associated larger value of OH results in a higher RO_2 (4.6×10^{10} molec cm^{-3}), lower NO (7 ppt) and similar HO_2 (2.3×10^9 molec cm^{-3}). The result is a much smaller chemical production of ANs (7 ppt), and a

net gradient of –4 ppt from the combined effects of deposition and chemical production, a value smaller than inferred from the observations but at least with the same sign. Gradients calculated from both residence times/OH values are less negative than observed, implying that net chemical production is smaller than we calculate using a reaction mechanism that treats ΣANs as stable unreactive products of the RO_2+NO reaction.

A much smaller net chemical production of ΣANs may occur if some fraction of the reactions of OH with ΣANs produce either HNO_3 or NO_2 (R11a,b) instead of a chemically more complex AN (R11c):

$$RONO_2 + OH \rightarrow HNO_3 + R'O \quad \text{(R11a)}$$

$$\rightarrow\rightarrow NO_2 + RO(OH) \quad \text{(R11b)}$$

$$\rightarrow\rightarrow H_2O + R'ONO_2 \quad \text{(R11c)}$$

Direct laboratory evidence for the products of R11 is sparse and equivocal (Nielsen et al., 1991; Treves and Rudich, 2003), and global and regional models that represent organic nitrate chemistry in detail use branching fractions ranging from 0 to 100% (Horowitz et al., 1998; Poschl et al., 2000 and references therein). Assuming an effective rate constant of 4.5×10^{-11} cm^3 molec^{-1} s^{-1} for the reaction of ΣANs with OH (Horowitz et al., 2006) requires the combined yield of R11a and b to be 0.06 (resulting in conversion of 6% of the ΣANs reacting with OH to NO_2 or HNO_3) to reduce the net chemical production from 28 ppt (gross production) to the observed 1 ppt and have the sum of deposition and net chemical production be consistent with the inference of a ∼–10 ppt gradient for a 420 s residence time. For a 70 s residence and the larger associated OH we require a much larger yield of NO_2 and HNO_3, 30%. Even this larger 30% value is less than what is used in global models; for example, a 40% yield for R11b is assumed in the model of Horowitz et al. (2006). If the 6–30% range in yields were true for ΣANs above the canopy as well, it implies a lifetime of ΣANs in the boundary layer of 4 to 20 h at noon equivalent OH (5×10^6 molec cm^{-3}). During August 2004 (Fig. 1), we observe rapid changes in ΣAN mixing ratio above the canopy that are more consistent with a short chemical lifetime (∼hours). However, we note that ΣANs represent a wide range of chemical species and that assuming that these species have a single chemical lifetime is probably not correct. More likely there is a set of short-lived compounds that quickly react away, leaving behind a longer-lived ΣAN population made up of different chemical species than the primary mixture.

Unsaturated alkyl nitrates also react with O_3. Estimates for the rate constants for the reaction of isoprene nitrates with O_3 range from 1–40×10^{-17} molec cm^{-3} s^{-1} (Giacopelli et al., 2005). If the higher end of this range is appropriate for the mix of ΣANs in the UC-BFRS canopy, then these reactions would constitute a rapid sink of ΣANs if, by analogy to R11a,b, the products are not alkyl nitrates. Including the effect of loss to O_3 reactions would lower the yield required for the OH reactions, but would not change the apparent lifetime of ΣANs, which is most directly constrained by the measurements.

These mechanisms affecting the ΣAN flux have a slight feedback to our assessment of within-canopy OH. For example, if the 6%–30% yield inferred above occurred entirely via R11a and was thus a large source of within-canopy HNO_3, with the balance an increasingly functionalized ΣAN (R11c), the OH required for the data to be consistent with the HNO_3 flux measurements and a 400 s residence time would be about 80% of the value inferred assuming OH-NO_2 reactions are the only HNO_3 source. This is an important quantitative point; however, it has no effect on the qualitative conclusion that within-canopy OH during the summer at UC-BFRS is much higher than the OH at the 14.3 m measurement height.

5.3 ΣPNs

The oxidation of ketones or aldehydes by either OH or O_3 produces peroxy acyl ($RC(O)O_2$) radicals, which react with NO_2 to produce peroxy acyl nitrates (PNs),

$$OH + \text{aldehydes} \xrightarrow{NO_2} PNs \quad \text{(R12)}$$

For example, the oxidation of acetaldehyde (CH_3CHO) followed by reaction with NO_2 produces peroxy acetyl nitrate (PAN), a molecule that is expected to represent 70–80% of the ΣPNs observed at UC-BFRS. The lifetime of acetaldehyde with respect to 3×10^7 molec cm^{-3} OH is 2.4×10^3s, short enough to produce a considerable amount of PAN within the 400 s canopy residence time. Unlike HNO_3, PNs have rapid chemical sources and sinks, so we cannot approximate the increase in ΣPNs in the canopy as equal to their integrated production over 400 s:

$$OH + \text{acetaldehyde} \rightarrow PA \quad \text{(R13)}$$

$$PA + NO_2 \rightarrow PAN \quad \text{(R14)}$$

$$PAN \rightarrow PA + NO_2 \quad \text{(R15)}$$

$$PA + NO \rightarrow \text{products} \quad \text{(R16)}$$

$$PA + HO_2 \rightarrow \text{products} \quad \text{(R17)}$$

$$PA + RO_2 \rightarrow \text{products} \quad \text{(R18)}$$

where PA is the peroxy acetyl radical. Most PNs have similar chemistry to PAN, and we use this chemistry as a surrogate for the chemistry of ΣPNs in the calculation below.

As above, we scale the winter V_{dep} for ΣPNs using the observed friction velocity to estimate the summertime V_{dep} of 1.1 cm s^{-1}. Then we use this number to calculate the ΣPN deposition flux. If deposition occurred without a chemical

source of ΣPNs, the concentration at 7 m would be –13 ppt lower than at 14.3 m. The net chemical production of 21 ppt of ΣPNs required by the flux measurements can be expressed as:

$$P_{PAN} = \int (k_{14}\,[PA]\,[NO_2] - k_{15}\,[PAN])d\tau \quad (14)$$

The canopy residence time (τ) is not long enough for PAN to reach steady state, but we assume PA radicals reach steady state:

$$PA_{ss} = \frac{k_{13}\left[\text{acetaldehyde}\right][OH] + k_{15}\,[PAN]}{k_{14}\,[NO_2] + k_{16}\,[NO] + k_{17}\,[HO_2] + k_{18}\,[RO_2]} \quad (15)$$

We solve for OH by substituting Eq. 15 into Eq. 14 and integrating for 400 s. We use concentrations of 2.5 ppb for acetaldehyde, 0.758 for PAN, 0.311 for NO_2, 0.028 ppb for NO, 2.5×10^9 molec cm^{-3} for HO_2, 1.2×10^{10} molec cm^{-3} for RO_2 with k_{16}=1.29×10^{-11} cm^3 molec^{-1} s^{-1} and k_{17}=1.1×10^{-11} cm^3 molec^{-1} s^{-1}, the rate for PA radicals with CH_3O_2 (Tyndall et al., 2001). We calculate 3.2×10^7 molecules OH cm^{-3} are present at 7 m with a 420 s residence time, producing the observed ΣPN gradient. The shorter 70 s residence time, and accompanying increased RO_2 described above, results in a 16×10^7 molec OH cm^{-3}. These OH predictions are nearly identical to the 2.8 to 16×10^7 molec cm^{-3} (420 to 70 s residence times) we derive from the HNO_3 measurements. Given the assumptions and uncertainties, this near exact agreement is no doubt fortuitous. However, the overall consistency is reassuring.

The predicted ΣPNs gradients highlight the balance between above-canopy mixing ratios, deposition and within-canopy chemistry. For example, the observed mixing ratio of ΣPNs above the canopy is 750 ppt, deposition is calculated to produce a negative gradient of 13 ppt and the rather rapid chemistry inferred represents a source of 21 ppt, overcoming this negative gradient to produce a positive gradient of 8 ppt. These two terms are in close balance – if the above canopy concentration were double or the deposition were twice as fast the sign of the flux would be reversed. Such variations are within the range of prior reports of deposition velocities and concentrations for ΣPNs.

5.4 NO_x and NO_y

We expect emissions and chemistry to be affecting the flow of NO_x into and out of the canopy significantly and thus, for analysis of the summer NO_x fluxes, we cannot reasonably assume that the NO_x flux is zero as we did for winter. Instead, we calculate the concentrations and fluxes of NO using a combination of the steady state relationships connecting NO and NO_2, the attenuation of J_{NO_2} derived from the winter observations and a calculation of the HO_2 and RO_2 concentrations that are consistent with the 14.3 m (5.7×10^6 molec cm^{-3}) and 7 m (2.8×10^7 molec cm^{-3}) canopy OH and the 8.4 s^{-1} OH lifetime. Using the steady-state model described above, we calculate the NO mixing ratio at 7 m was 19 ppt, and at 14.3 m was 45 ppt. The observed 300 ppt NO_2 above the canopy is thus associated with an NO to NO_2 ratio of 0.15 and a total NO_x of 345 ppt. This ratio is 20% lower than the 0.18 seen in prior observations by Day et al. (2006) at this site (although within the ±15 ppt uncertainty of the NO measurement). At 7 m a.g.l., we calculate NO_x of 330 ppt, and a NO:NO_2 ratio of 0.06. Using these numbers and the CO_2 similarity approach to deriving a flux from a gradient, we calculate an NO flux of –16 ppt m s^{-1} at 14.3 m a.g.l. The NO_x flux, calculated as the sum of the observed NO_2 flux of 7 ppt m s^{-1} and the calculated NO flux of –16 ppt m s^{-1}, is –9 ppt m s^{-1}. If there were no chemical removal of NO_x, we would expect more NO_x within the canopy than above because of NO_x emissions from the soils in the region. This would result in a net upward flux of NO_x – a result that is opposite in sign to what we infer. The fact that we calculate less NO_x and an associated net downward NO_x flux is strong supporting evidence for the chemical conversion of NO_x to higher oxides that we infer above. This is one of the key predictions of our analysis, one that should be tested with simultaneous observations of the NO and NO_2 fluxes and gradients.

The chemistry producing HNO_3, ΣANs, and ΣPNs described above removes NO_x from the canopy; in the absence of ecosystem NO_x emissions, this chemical conversion of NO_x to NO_z (NO_y – NO_x) would produce a gradient in NO_x of –54 ppt, shown as a dashed line in Fig. 4c. However, the decrease in NO_x of 15 ppt at 7 m is only ∼25% of the decrease we calculate based on oxidation of NO_x to ΣPN, ΣANs and HNO_3. This difference implies a large NO_x emission source.

Before examining the possible NO_x sources, it is useful to consider the NO_y flux. ΣNO_{yi} at Blodgett Forest was 1.6 ppb at noon during August 2004. Assuming the NO_y flux is the sum of the NO flux we calculate and the fluxes of the four classes of species we observe directly, we calculate a net NO_y flux of –5 ppt m s^{-1} (–2.9 ng(N) m^{-2} s^{-1}). NO_y flux measurements at other sites range from –3.4 ppt m s^{-1} at Schefferville, Quebec, where NO_y was 0.24 ppb, to –23.2 ppt m s^{-1} at Harvard Forest, where NO_y varied in the range 1.9 to 4.7 ppb (Munger et al., 1996). These prior observations have been interpreted using estimates of HNO_3 fluxes based on concentration measurements (such as Eq. 9). Our results indicate some consistency in the total fluxes at the different sites, but suggest that the underlying mechanisms may be much more complex. That is, the flux-concentration relationship we observe for total NO_y is not unusual, rather the decomposition into individual terms obtained using eddy covariance is.

Returning to the question of the NO_x flux, the –5 ppt m s^{-1} NO_y flux at the top of the canopy must be equal not only to the sum of the observed NO_{yi} fluxes, but also to the sum of gross fluxes we calculate for exchange

between the atmosphere and the forest. Exchanges between the atmosphere and the forest are the deposition terms we calculated above from the exchange velocities; gross deposition is calculated to be –32 ppt m s^{-1}, the sum of HNO_3 (–17 ppt m s^{-1}), ΣANs (–6.7 ppt m s^{-1}), and ΣPNs (–8.3 ppt m s^{-1}) deposition. If the flux into the forest at the top of the canopy is only –5 ppt m s^{-1}, this deposition flux implies that 27 ppt m s^{-1} (∼15 ng(N) m^{-2} s^{-1}) is emitted from the forest and rapidly converted to NO_x.

The only candidates for ecosystem NO_x emission we are aware of are emission of NO, NO_2 and nitrous acid (HONO). Microbial activity in soils causes NO emissions, which depend on soil type, temperature, moisture, and nitrogen content (Williams et al., 1992). NO is then rapidly converted to NO_2 by reaction with O_3. While no data are available for soil NO_x emissions at UC-BFRS, measurements of soil NO_x emissions in the oak forests of the Sierra Nevada foothills to the west showed fluxes in the range of 5.8 to 15 ppt m s^{-1} in the summer (Herman et al., 2003). Soil emissions at UC-BFRS, which receives less N-deposition because of its greater distance from the urban source region, are expected to be lower. An upward NO_x flux at the low end of this range of 5.8 ppt m s^{-1} (2.9 ng(N) m^{-2} s^{-1}) would account for 20% of the 27 ppt m s^{-1} NO_x emissions that are required to balance the NO_y flux budget. A flux of 15 ppt m s^{-1} would account for over 50% of the NO_x emissions we infer.

Other known NO_x sources from ecosystems are those associated with compensation points for NO and NO_2 and those associated with HONO fluxes. Direct NO_2 emissions from plants that are below their NO_2 compensation point, the atmospheric mixing ratio above which molecules are deposited to plants and below which emission occurs, have been reported by Sparks et al. (2001) who observed compensation points for tropical plants in the range of 0.5–1.6 ppb, and Rondon and co-workers (Rondon et al., 1993; Rondon and Granat, 1994) who found coniferous trees exhibited compensation points in the range of 0.1–0.7 ppb. NO_2 mixing ratios are at or below all but the lowest of these thresholds at UC-BFRS. Using a leaf area index of 6 (Holzinger et al., 2005a), and an emission rate of 3.6 pmol NO_2 m^{-2} s^{-1} (Sparks et al., 2001) when below the compensation point, plants at UC-BFRS are calculated to emit 0.5 ppt m s^{-1} (0.3 ng(N) m^{-2} s^{-1}). This is <2% of the inferred NO_x flux; thus unless ponderosa pines are much stronger NO_2 emitters than plants previously studied, NO_2 emission as a result of being below the compensation point is unlikely to account for the NO_x flux we infer. NO has a separate compensation point. Studies of NO emissions from spruce trees found an NO:CO_2 flux ratio of -4.1×10^{-6} (Wildt et al., 1997); extrapolation to the ponderosa pine plantation at UC-BFRS suggests that direct plant emissions of NO could account for a flux of 0.87 ppt m s^{-1}, again too small (3% of the needed source) to account for the inferred fluxes. Both sources of NO_x emissions should certainly be examined with more direct leaf and plant level experiments to help clarify the mechanisms at work in the UC-BFRS ecosystem.

Another possible contribution to NO_x fluxes is UV-induced NO_x or HONO production, presumably from nitrate on leaves. For example, Raivonen et al. (2006) report UV-induced emission of NO_x of as much as 1.7 ppt m s^{-1}. Elevated HONO has recently been observed in forest canopies, possibly the result of heterogeneous reactions of deposited N on canopy surfaces. Kleffmann et al. (2005) suggested that daytime HONO production of up to 500 ppt hr^{-1} that could not be explained by gas-phase chemistry alone was occurring in a forest canopy. Note that HONO is not detected by the TD-LIF as it thermally dissociates to NO, not NO_2 (Perez et al., 2007). HONO is rapidly photolyzed, and thus potentially provides a source of both OH and NO radicals ($\tau_{HONO}\approx600$ s above the canopy at Blodgett), as well as a mechanism for deposited HNO_3 to be returned to the atmosphere as NO_x (e.g. Zhou et al., 2003). Assuming this process were occurring at the same rate at UC-BFRS as in the Kleffmann experiment, and that half of the HONO produced is converted to NO before transport out of the canopy, this production would contribute approximately 20 ppt m s^{-1} and account for 74% of the inferred NO_x flux. Even a source 10 times smaller would be a significant contributor to the overall nitrogen budget, although HONO itself would have a mixing ratio of only a few ppt.

In addition to the above mechanisms, we note several other possibilities for balancing the flux budget, including systematic errors 1) in the measurements, 2) in the above-canopy NO estimate, 3) in the estimated V_{dep}, 4) in the estimate of RO_2 and HO_2 and 5) associated with the assumptions of our micrometeorological analyses. Neither of the first two possible sources of error is large enough by itself to affect our conclusions substantially. Systematic errors in the TD-LIF flux measurements may be as much as 20% (Farmer et al., 2006). Reducing all of the observed summer fluxes by 20% reduces the derived ecosystem NO_x emission by 15% to 23 ppt m s^{-1} (13 ng(N) m^{-2} s^{-1}). If the above-canopy NO is larger than we calculate, we would be underestimating the NO deposition flux. Increasing the above-canopy NO to NO_2ratio from 0.15 to the 0.18 previously observed at UC-BFRS results in greater net NO_y deposition (–9 ppt m s^{-1}), and a lower ecosystem emission of 19 ppt m s^{-1} (∼11 ng(N) m^{-2} s^{-1}).

The third term, estimates of V_{dep}, is one of the key factors driving the need for large NO_x fluxes. If we reduce the V_{dep} terms by 50%, the inferred OH would be 1.2×10^7 cm^{-3}, the NO_x emission flux into the canopy would be one half of what we calculate in the standard case: 14 ppt m s^{-1} (7 ng(N) m^{-2} s^{-1}). This could be accounted for by a combination of soil emissions, a small HONO source and small errors in the flux measurements or estimates of NO. Lower values for V_{dep} than we calculate have been reported previously. For example, wet leaf surfaces, which occur during the wet Sierra Nevada winters, can increase deposition of PAN (Turnipseed et al., 2006). Since our estimates for summer are

based on scaling the winter numbers, we might be overestimating PAN deposition. However, such a large reduction in the HNO_3 deposition velocity is unlikely.

The fourth item would reinforce or could be a more effective alternative to the second one, errors in the above-canopy NO estimate. Although our calculations already suggest very high OH, RO_2 and HO_2 in the canopy, results and analysis by Thornton et al. (2002) and the laboratory measurements of Hasson et al. (2004) have suggested that RO_2 and HO_2 loss rates are overestimated, possibly because oxygenated RO_2 react with HO_2 to regenerate OH instead of forming a soluble peroxide that is removed by deposition. If this is the case, then higher within-canopy RO_2 and HO_2 would cause a steeper gradient in NO, and thus increased ΣNO_{yi} deposition, reducing the need for additional NO_x emission sources.

Finally, all of the analysis in this paper assumes that the concentration of each NO_{yi} species peaks at the same height, and that they are transported across gradients according to a single common similarity calculation. However, spectral analysis of each compound (Fig. 5) suggests that vertical profiles of measured species are not identical, and that each is carried by turbulent eddies of different lengths, a fact which may mean that our assumption that both the fluxes and the chemistry must balance at a single height is too strict a constraint. Although there is some discussion of use of cumulative cospectra, or ogives, to relate fluxes of conserved tracers to source locations, we are not aware of any precedent for quantitative interpretation of the ogives and certainly there is no precedent for quantitative interpretation of the ogives in a situation where there is chemcial flux divergence. If our zero-order model is correct, then the ogives will include effects of deposition and of chemical production. These two terms are different for the different species and are not necessarily contributing equally to the flux at all frequencies. For example, for HNO_3 we calculate a gradient due to deposition of –27 ppt and chemical production of +35 ppt. These numbers are approximately 5% and 8% of the 500 ppt concentration and they result in a net increase of HNO_3 of about 1%, or +4ppt within the canopy. For comparison, the ΣPN gradient due to deposition is about ½ the magnitude of that due to HNO_3 and the chemical production 2/3 the magnitude corresponding to 2% and 3% of the 750 ppt above canopy ΣPNs. Further, the ΣPN production depends on reaction of aldehydes with OH and then subsequent addition of NO_2 whereas HNO_3 production occurs in a single step. Thus we might expect that the source term for chemical production of PNs and HNO_3 will have a slightly different spectral distribution because the production and removal terms occur at different heights for each chemical species and not necessarily at the same height for the different species. As a result of these different factors, the ogives that represent both the effects of the sinks and the sources will change sign from upward to downward at different frequencies. Consistent with this qualitative discussion, both the cospectra and ogives exhibit upward and downward fluxes being carried at different frequencies, as

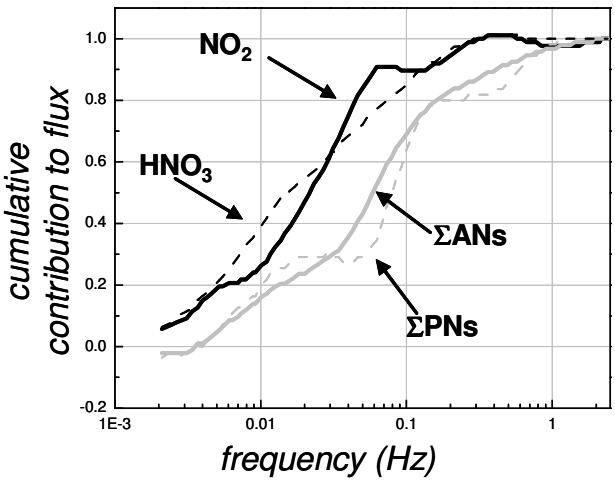

Fig. 5. Ogive plot (cumulative contribution to flux as a function of frequency) of TD-LIF data for all day-time half hours from 1-10 August 2004. As the ogive plateaus at high frequencies for all species, the TD-LIF is fast enough (5 Hz) to capture all relevant flux-carrying eddies. Differences in ogive structure between the NO_{yi} species may be attributable to different vertical profiles, the result of production and loss processes occurring at different heights in the canopy.

exemplified in the dip in the PNs ogive around 0.05 Hz, signifying a change in flux sign. Similar markers are present in the NO_2 (0.007 Hz and 0.01 Hz) and ΣAN (0.02 Hz) ogives. However, we do not believe that differences in the ogives can be used to support or contradict our hypothesis with much confidence at this point in time. In our opinion, a direct calculation using large eddy-simulation to predict the spectral distribution of the chemical fluxes will be required to interpret the ogives. To more fully address whether and to what extent this approximation of similar vertical profiles does affect the inferred fluxes, a more detailed canopy model representing transport and chemistry must be developed.

5.5 Discussion

As we have described, the observations of HNO_3, ΣANs, ΣPNs, and NO_2 fluxes are self-consistent if we draw several conclusions about the chemistry occurring within the forest canopy. Chief among these is that for a 400 s residence time the OH is of the order 3×10^7 molecules cm^{-3} within the canopy, a factor of 5 larger than it is above the canopy. This conclusion should clearly be tested by observations.

High OH concentrations within the UC-BFRS canopy have previously been suggested by Goldstein and coworkers (Goldstein et al., 2004; Holzinger et al., 2005b). In these papers, Goldstein et al. have taken three nominally independent points of view regarding the production of OH. They calculate OH production rates based on the removal rate of O_3, based on the reactivity of observed VOC, and based on

the observation of molecules presumed to be products of VOC reaction with O_3. These routes all result in an estimate of the rate of O_3 reaction with VOC ($k_1[O_3][VOC]$) in the UC-BFRS canopy of about 7×10^8 reactions cm^{-3} s^{-1}. Beginning with this estimate, the major unknowns required for estimating OH in steady-state are the OH loss rate and the yield of OH from R1. As described above, the OH loss rate, $\Sigma k_i[VOC_i]$=8.4 s^{-1}, can be derived from previous VOC observations at UC-BFRS (Lamanna and Goldstein, 1999) scaled by a "missing reactivity" factor (Di Carlo et al., 2004). Here we assume a 30% OH yield for R1. Then, assuming steady state, and that the HO_2+NO reaction is a small source by comparison,

$$P_{OH}=\alpha_1 k_1[VOC][O_3]=0.3\times7\times10^8 molec cm^{-3} s^{-1} \quad (16)$$

$$L_{OH} = k_{OH+VOC}[VOC][OH] = 8u4g^{-1} \times OH \quad (17)$$

Solving for OH, we calculate 2.4×10^7 molec OH cm^{-3} (an estimate that is independent of residence time). This number is of the same order as our estimates based on the HNO_3 and ΣPN fluxes of 2.7 and 2.8×10^7 molec cm^3, respectively, calculated for a 420 s residence time, and a factor of 5 smaller than our estimates based on the fluxes and a 70 s residence time. Goldstein et al. (2004) presented a similar calculation for the UC-BFRS canopy, and explored some of the factors in the above analysis that are not well known to arrive at a range of 0.8–3×10^7 molec cm^{-3} OH averaged over the full 12.5 m between the forest floor and their observation point above the canopy. Our observations suggest that the concentration in the region of the canopy contributing to upward fluxes of nitrogen oxides is at the high end of this range.

In the only model we know of examining the chemical consequences of sesquiterpene emissions, Stroud et al. (2005) conclude O_3 reactions can increase within-canopy OH from 5×10^5 to 1×10^6 molec cm^{-3} for terpenoid emissions comparable to those implied by O_3 flux measurements at UC-BFRS. That study used OH yields for β-caryophyllene (6%), which are at the low end of the reported range for OH yields from sesquiterpenes (e.g. Atkinson et al., 1992; Shu and Atkinson, 1994). Our observations suggest the OH yields are much higher, and that enhanced within-canopy reactivity might be a general characteristic of pine forests and other ecosystems where very reactive terpene emissions are substantial.

At this point in time, our understanding of terpenoid emissions, OH yields, etc. is inadequate for an accurate extrapolation from our results to the effects of within canopy OH on a global scale. However, recent advances in technologies for observing very reactive VOC are beginning to provide data that might be used in an extrapolation. For example, studies show that variability in sesquiterpene emissions depends on plant species and varies with season, that pine tree sesquiterpene emissions can be temperature and light dependent, and that sesquiterpene emissions are strong enough to significantly impact secondary organic aerosol formation (Helmig et al., 2006; Holzke et al., 2006; Helmig et al., 2007). At this point, pine forests (especially ones in warmer climates) appear to be particularly good candidates for sesquiterpene emissions that lead to high within-canopy OH.

Although much more research is required to assess the global effects of high within-canopy OH, the high OH we show is present within the canopy airspace at UC-BFRS, and suggest might be present in many pine forests, will no doubt have interesting and possibly important consequences for the mechanisms of regional atmospheric chemistry, biosphere-atmosphere exchange of nitrogen, production of secondary organic aerosols, and determining the identity of VOC that are emitted at the ecosystem scale. One example of the consequences of high within-canopy OH is the increase in the boundary layer average OH. Assuming a 1 km boundary layer, a 5-fold increase in OH confined to 10 m corresponds with a 5% increase in overall oxidation rates of NO_x and VOC. As the more oxidized forms of NO_y are more soluble than NO_x, they deposit to forest ecosystems faster than NO and NO_2. Thus somewhat paradoxically, the upward HNO_3 flux we observe is evidence for a 5% faster regional deposition of HNO_3. If mature pine forests emit reactive BVOC in proportion to their height, then this mechanism could easily increase oxidation rates by more than 10% along the western slopes of the Sierra Nevada. These effects could be important in assessing the spatial extent of regional ozone and in comparing models to ground-based or satellite observations of NO_2. Another example of potential ramifications of high OH is evidenced by comparison of OH and O_3 VOC oxidation rates, which suggest that about half the VOC oxidation occurring within the UC-BFRS canopy is due to reaction with OH and not with O_3, a result that should have testable implications for the distribution of VOC products. For example, Lee et al. (2006) showed that some of the masses identified by PTR-MS are produced during oxidation of terpenoids by OH, but not O_3.

The high within-canopy OH that we show is present in the UC-BFRS canopy implies that many of the compounds emitted by leaves will be oxidized by OH before they are observed as ecosystem-scale fluxes. It is already well known that sesquiterpenes are removed by ozone prior to escape from canopies because their chemical lifetime is seconds (Ciccioli et al., 1999). High OH concentrations imply that in addition there is substantial oxidation of species with slower reaction rates to O_3, and that reaction products such as acetone and acetaldehyde, which are important for the global HO_x budget may be observed in emission at the ecosystem-scale but, at least in part, be secondary products that are the result of VOC-OH reactions, and not primary biogenic emissions. For example, MBO, which is a primary emission from ponderosa pines at UC-BFRS, has a lifetime of about 700 s with respect to 2×10^7 molec cm^{-3} OH. Oxidation of MBO by OH produces acetone with 50% yield (Ferronato et al.,

1998). Since 700 s is comparable to the canopy residence time, within-canopy reactions of MBO may contribute substantially to the acetone flux observed above the canopy by Schade and Goldstein (2001).

In addition to accelerating oxidation rates, the localized nature of the high OH may increase the probability of forming secondary organic aerosol (SOA) within forest canopies. High SOA over forests has been described by Tunved et al. (2006). SOA produced through the condensation of oxidized organic compounds is more likely to form when a high concentration of gas phase precursors is available. Locally high OH concentrations are one recipe for producing such high concentrations as multiple oxidation steps can all occur before dilution of precursors into the boundary layer above the canopy air space.

Finally we note that the oxidizing environment within forest canopies depends on O_3, NO_x and BVOC emissions that depend on light and exponentially on temperature. Since temperature, O_3 and NO_x have all increased since pre-industrial times, there have likely been increases in the extent to which rapid within-canopy chemistry is occurring. Much remains to be learned about the consequences of this chemistry for our understanding of the present and pre-industrial atmosphere and biosphere and the interactions between them.

6 Conclusions

We used eddy covariance measurements of NO_2, ΣPNs, ΣANs and HNO_3 to probe the mechanisms controlling biosphere-atmosphere exchange, obtaining surprising results that would not have been observed from more commonly used instrumentation and flux measurement techniques. During summer we observed upward fluxes of HNO_3 and ΣPNs and downward fluxes of ΣANs, and we inferred downward fluxes of NO_x above the ponderosa pine plantation at UC-BFRS. Contrasting these results with winter observations, which are consistent with our expectations (i.e., all of the higher oxides are observed to be depositing and NO_x fluxes are near zero), leads us to conclude that high (3×10^7 molec cm^{-3}) within-canopy OH is driving the upward fluxes during summer. These results show that mechanisms controlling NO_y fluxes – and, by implication, many other forest processes – are more complex than previously thought. Although this analysis shows that the high within-canopy OH hypothesis is plausible and consistent with a wide range of data, it also requires several inferences to be made about processes that are not well known at this time. First, we infer that reactions of ΣANs with OH produce NO_2 or HNO_3 with a yield of 6–30%. The results also require that there be large emissions of NO_x into the canopy. These fluxes can be explained by a combination of NO_x fluxes from soil in the range of previous observations in the region and a large additional source. HONO production on canopy surfaces, as has been reported in recent experiments, would be consistent with this additional source. The size of the NO_x flux, and thus the size of the required HONO emissions, can be reduced if there are errors in our understanding of the deposition velocity of HNO_3, or if errors in the current understanding of peroxy radical chemistry result in steeper NO gradients. Either mechanism reduces the required NO_x flux. Alternatively, we note that a more sophisticated analysis of the data than we have yet developed, one capable of addressing the differences in the spectral properties of the fluxes of different NO_y species might result in a different interpretation of the flux balance. While further studies and measurements are clearly required to investigate within-canopy chemistry and the mechanisms proposed in this paper, the predicted gradients are small, making the gradient observations particularly challenging.

Finally, taking these caveats and uncertainties into account does not change the basic conclusion of this paper – that there is much higher OH within the UC-BFRS canopy than above, and that the NO_{yi} fluxes we describe and the OH we derive from these fluxes and a 400 s residence time are consistent with OH inferred from O_3 and VOC fluxes. The calculated values for OH are inconsistent with what we would derive if the residence time is 70 s unless the ΣAN oxidation by OH is a large source of HNO_3 within the canopy, a possibility that will require much further study.

Acknowledgements. We acknowledge NSF for funding (grant ATM-0138669 and ATM 0639847), Allen Goldstein and coworkers for CO_2 data, Dennis Baldocchi for helpful conversations, and thank the staff of UC-BFRS for support.

Edited by: A. B. Guenther

References

Atkinson, R., Aschmann, S. M., Carter, W. P. L., Winer, A. M., and Pitts, J. N.: Alkyl nitrate formation from the NO_x-air photooxidations of C_2-C_8 n-alkanes, J. Phys. Chem., 86, 4563–4569, 1982.

Atkinson, R., Aschmann, S. M., Arey, J., and Shorees, B.: Formation of OH radicals in the gas-phase reactions of O_3 with a series of terpenes, J. Geophys. Res., 97, 6065–6073, 1992.

Bauer, M. R., Hultman, N. E., Panek, J. A., and Goldstein, A. H.: Ozone deposition to a ponderosa pine plantation in the Sierra Nevada Mountains (CA): A comparison of two different climatic years, J. Geophys. Res., 105, 22 123–22 136, 2000.

Bertram, T. H. and Cohen, R. C.: A prototype instrument for the detection of semi-volatile organic and inorganic nitrate aerosol, Eos Trans. AGU, 84, 2003.

Bertram, T. H.: Observational constraints for the source strengths, transport and partitioning of reactive nitrogen on regional and global scales, PhD thesis, University of California, Berkeley, Berkeley, 2006.

Brost, R., Delany, A., and Huebert, B.: Numerical modeling of concentrations and fluxes of HNO_3, NH_3 and NH_4NO_3 near the surface, J. Geophys. Res., 93, 7137–7152, 1988.

Brown, S. S., Dibb, J. E., Stark, H., Aldener, M., Vozella, M., Whitlow, S., Williams, E. J., Lerner, B. M., Jakoubek, R., Middlebrook, A. M., DeGouw, J. A., Warneke, C., Goldan, P. D., Kuster, W. C., Angevine, W. M., Sueper, D. T., Quinn, P. K., Bates, T. S., Meagher, J. F., Fehsenfeld, F. C., and Ravishankara, A. R.: Nighttime removal of NO_x in the summer marine boundary layer, Geophys. Res. Lett., 31, L07108, doi:10.1029/2004GL019412, 2004.

Carroll, J. J. and Dixon, A. J.: Regional scale transport over complex terrain, a case study: tracing the Sacramento plume in the Sierra Nevada of California, Atmos. Eniviron., 36, 3745–3758, 2002.

Carslaw, N., Creasey, D. J., Harrison, D., Heard, D. E., Hunter, M. C., Jacobs, P. J., Jenkin, M. E., Lee, J. D., Lewis, A. C., Pilling, M. J., Saunders, S. M., and Seakins, P. W.: OH and HO_2 radical chemistry in a forested region of north-western Greece, Atmos. Eniviron., 35, 4725–4737, 2001.

Ciccioli, P., Brancaleoni, E., Frattoni, M., Di Palo, V., Valentini, R., Tirone, G., Seufert, G., Bertin, N., Hansen, U., Csiky, O., Lenz, R., and Sharma, M.: Emission of reactive terpene compounds from orange orchards and their removal by within-canopy processes, J. Geophys. Res., 104, 8077–8094, 1999.

Cleary, P. A., Murphy, J. G., Wooldridge, P. J., Day, D. A., Millet, D. B., McKay, M., Goldstein, A. H., and Cohen, R. C.: Observations of total alkyl nitrates within the Sacramento Urban Plume, Atmos. Chem. Phys. Discuss., 5, 4801–4843, 2005, http://www.atmos-chem-phys-discuss.net/5/4801/2005/.

Collins, W. J., Derwent, R. G., Johnson, C. E., and Stevenson, D. S.: The oxidation of organic compounds in the troposphere and their global warming potentials, Clim. Change, 52, 453–479, 2002.

Day, D. A., Wooldridge, P. J., Dillon, M. B., Thornton, J. A., and Cohen, R. C.: A thermal dissociation laser-induced fluorescence instrument for in situ detection of NO_2, peroxy nitrates, alkyl nitrates, and HNO_3, J. Geophys. Res., 107, 4046, doi:10.1029/2001JD000779, 2002.

Day, D. A.: Observations of NO_2, total peroxy nitrates, total alkyl nitrates, and HNO_3 in the Mid-Sierras and Sacramento plume using Thermal Dissociation-Laser Induced Fluorescence, PhD thesis, University of California, Berkeley, Berkeley, 2003.

Day, D. A., Dillon, M. B., Wooldridge, P. J., Thornton, J. A., Rosen, R. S., Wood, E. C., and Cohen, R. C.: On alkyl nitrates, O_3, and the "missing NO_y", J. Geophys. Res., 108(D16), 4501, doi:10.1029/2003JD003685 , 2003.

Day, D. A., Wooldridge, P. J., and Cohen, R. C.: Observations of the temperature dependence of HNO_3, ΣANs, ΣPNs, and NO_2, Atmos. Chem. Phys., 8, 1867–1879, 2008, http://www.atmos-chem-phys.net/8/1867/2008/.

Di Carlo, P., Brune, W. H., Martinez, M., Harder, H., Lesher, R., Ren, X. R., Thornberry, T., Carroll, M. A., Young, V., Shepson, P. B., Riemer, D., Apel, E., and Campbell, C.: Missing OH reactivity in a forest: Evidence for unknown reactive biogenic VOCs, Science, 304, 722–725, 2004.

Dillon, M. B., Lamanna, M. S., Schade, G. W., Goldstein, A. H., and Cohen, R. C.: Chemical evolution of the Sacramento urban plume: Transport and oxidation, J. Geophys. Res., 107, 4045, doi:10.1029/2001JD000969, 2002.

Donahue, N. M., Kroll, J. H., Anderson, J. G., and Demerjian, K. L.: Direct observation of OH production from the ozonolysis of olefins, Geophys. Res. Lett., 25, 59–62, 1998.

Doskey, P. V., Kotamarthi, V. R., Fukui, Y., Cook, D. R., Breitbeil, F. W., and Wesely, M. L.: Air-surface exchange of peroxyacetyl nitrate at a grassland site, J. Geophys. Res., 109, 13 153–13 168, 2004.

Faloona, I., Tan, D., Brune, W., Hurst, J., Barket, D., Couch, T. L., Shepson, P., Apel, E., Riemer, D., Thornberry, T., Carroll, M. A., Sillman, S., Keeler, G. J., Sagady, J., Hooper, D., and Paterson, K.: Nighttime observations of anomalously high levels of hydroxyl radicals above a deciduous forest canopy, J. Geophys. Res., 106, 24 315–24 333, 2001.

Farmer, D. K., Wooldridge, P. J., and Cohen, R. C.: Application of thermal-dissociation laser induced fluorescence (TD-LIF) to measurement of HNO_3, Σalkyl nitrates, Σperoxy nitrates, and NO_2 fluxes using eddy covariance, Atmos. Chem. Phys., 6, 3471–3486, 2006, http://www.atmos-chem-phys.net/6/3471/2006/.

Ferronato, C., Orlando, J. J., and Tyndall, G. S.: Rate and mechanism of the reactions of OH and Cl with 2-methyl-3-buten-2-ol, J. Geophys. Res., 103, 25 579–25 586, 1998.

Fiore, A. M., Horowitz, L. W., Purves, D. W., Levy, H., Evans, M. J., Wang, Y. X., Li, Q. B., and Yantosca, R. M.: Evaluating the contribution of changes in isoprene emissions to surface ozone trends over the eastern United States, J. Geophys. Res., 110, 12303, doi:10.1029/2004JD005485, 2005.

Fischer, M. and Littlejohn, D.: M. L. Fischer and D. Littlejohn, : Ammonia at Blodgett Forest, Sierra Nevada, USA, Atmos. Chem. Phys. Discuss., 7, 14139–14169, 2007, http://www.atmos-chem-phys-discuss.net/7/14139/2007/.

Fitzjarrald, D. R. and Lenschow, D. H.: Mean Concentration and Flux Profiles for Chemically Reactive Species in the Atmospheric Surface-Layer, Atmos. Eniviron., 17, 2505–2512, 1983.

Forkel, R., Klemm, O., Graus, M., Rappengluck, B., Stockwell, W. R., Grabmer, W., Held, A., Hansel, A., and Steinbrecher, R.: Trace gas exchange and gas phase chemistry in a Norway spruce forest: A study with a coupled 1-dimensional canopy atmospheric chemistry emission model, Atmos. Eniviron., 40, 28–42, 2006.

Fuentes, J. D., Wang, D., Neumann, H. H., Gillespie, T. J., Den-Hartog, G., and Dann, T. F.: Ambient biogenic hydrocarbons and isoprene emissions from a mixed deciduous forest, J. Atmos. Chem., 25, 67–95, 1996.

Gao, W., Wesely, M. L., and Doskey, P. V.: Numerical Modeling of the Turbulent-Diffusion and Chemistry of NO_x, O_3, Isoprene, and Other Reactive Trace Gases in and above a Forest Canopy, J. Geophys. Res., 98, 18 339–18 353, 1993.

Giacopelli, P., Ford, K., Espada, C., and Shepson, P. B.: Comparison of the measured and simulated isoprene nitrate distributions above a forest canopy, J. Geophys. Res., 110, D01304, doi:10.1029/2004JD005123, 2005.

Goldstein, A. H., Hultman, N. E., Fracheboud, J. M., Bauer, M. R., Panek, J. A., Xu, M., Wi, Y., Guenther, A. B., and Baugh, W.: Effects of climate variability on the carbon dioxide, water and sensible heat fluxes above a ponderosa pine plantation in the Sierra Nevada (CA), Agric. Forest Met., 101, 113–129, 2000.

Goldstein, A. H., McKay, M., Kurpius, M. R., Schade, G. W., Lee, A., Holzinger, R., and Rasmussen, R. A.: Forest thinning experiment confirms ozone deposition to forest canopy is dominated by reaction with biogenic VOCs, Geophys. Res. Lett., 31, L22106, doi:10.1029/2004GL021259, 2004.

Guenther, A., Hewitt, C. N., Erickson, D., Fall, R., Geron, C., Graedel, T., Harley, P., Klinger, L., Lerdau, M., Mckay, W. A., Pierce, T., Scholes, B., Steinbrecher, R., Tallamraju, R., Taylor, J., and Zimmerman, P.: A Global-Model of Natural Volatile Organic-Compound Emissions, J. Geophys. Res., 100, 8873–8892, 1995.

Hasson, A. S., Tyndall, G. S., and Orlando, J. J.: A product yield study of the reaction of HO_2 radicals with ethyl peroxy ($C_2H_5O_2$), acetyl peroxy ($CH_3C(O)O_2$), and acetonyl peroxy ($CH_3C(O)CH_2O_2$) radicals, J. Phys. Chem. A, 108, 5979–5989, 2004.

Helmig, D., Ortega, J., Guenther, A., Herrick, J. D., and Geron, C.: Sesquiterpene emissions from loblolly pine and their potential contribution to biogenic aerosol formation in the Southeastern US, Atmos. Eniviron., 40, 4150–4157, 2006.

Helmig, D., Ortega, J., Duhl, T., Tanner, D., Guenther, A., Harley, P., Wiedinmyer, C., Milford, J., and Sakulyanontvittaya, T.: Sesquiterpene emissions from pine trees – Identifications, emission rates and flux estimates for the contiguous United States, Environ. Sci. Technol., 41, 1545–1553, 2007.

Herman, D. J., Halverson, L. J., and Firestone, M. K.: Nitrogen dynamics in an annual grassland: oak canopy, climate, and microbial population effects, Ecological Applications, 13, 593–604, 2003.

Holzinger, R., Lee, A., McKay, M., and Goldstein, A. H.: Seasonal variability of monoterpene emission factors for a ponderosa pine plantation in California, Atmos. Chem. Phys. Discuss., 5, 8791–8810, 2005a, http://www.atmos-chem-phys-discuss.net/5/8791/2005/.

Holzinger, R., Lee, A., Paw U, K. T., and Goldstein, A. H.: Observations of oxidation products above a forest imply biogenic emissions of very reactive compounds, Atmos. Chem. Phys., 5, 67–75, 2005b, http://www.atmos-chem-phys.net/5/67/2005/.

Holzke, C., Hoffmann, T., Jaeger, L., Koppmann, R. and Zimmer, W.: Diurnal and seasonal variation of monoterpene and sesquiterpene emissions from Scots pine (*Pinus sylvestris* L.), Atmos. Eniviron., 40, 3174-3185, 2006.

Horii, C. V., Munger, J. W., Wofsy, S. C., Zahniser, M., Nelson, D., and McManus, J. B.: Fluxes of nitrogen oxides over a temperate deciduous forest, J. Geophys. Res., 109, D08305, doi:10.1029/2003JD004326, 2004.

Horii, C. V., Munger, J. W., Wofsy, S. C., Zahniser, M., Nelson, D., and McManus, J. B.: Atmospheric reactive nitrogen concentration and flux budgets at a Northeastern US forest site, Agric. Forest Met., 133, 210–225, 2005.

Horowitz, L. W., Liang, J. Y., Gardner, G. M., and Jacob, D. J.: Export of reactive nitrogen from North America during summertime: Sensitivity to hydrocarbon chemistry, J. Geophys. Res., 103, 13 451–13 476, 1998.

Horowitz, L. W., Fiore, A. M., Milly, G. P., Cohen, R. C., Perring, A., Wooldridge, P. J., Hess, P. G., Emmons, L. K., and Lamarque, J.-F.: Observational constraints on the chemistry of isoprene nitrates over the eastern United States, J. Geophys. Res., 112, D12S08, doi:10.1029/2006JD007747, 2007.

Huebert, B. J., Luke, W. T., Delany, A. C., and Brost, R. A.: Measurements of concentrations and dry surface fluxes of atmospheric nitrates in the presence of ammonia, J. Geophys. Res., 93, 7127–7136, 1988.

Kanakidou, M., Seinfeld, J. H., Pandis, S. N., Barnes, I., Dentener, F. J., Facchini, M. C., Van Dingenen, R., Ervens, B., Nenes, A., Nielsen, C. J., Swietlicki, E., Putaud, J. P., Balkanski, Y., Fuzzi, S., Horth, J., Moortgat, G. K., Winterhalter, R., Myhre, C. E. L., Tsigaridis, K., Vignati, E., Stephanou, E. G., and Wilson, J.: Organic aerosol and global climate modelling: a review, Atmos. Chem. Phys., 5, 1053–1123, 2005, http://www.atmos-chem-phys.net/5/1053/2005/.

Kastler, J., Jarman, W., and Ballschmiter, K.: Multifunctional organic nitrates as constituents in European and US urban photosmog, Fresen J Anal Chem, 368, 244–249, 2000.

Kleffmann, J., Gavriloaiei, T., Hofzumahaus, A., Holland, F., Koppmann, R., Rupp, L., Schlosser, E., Siese, M., and Wahner, A.: Daytime formation of nitrous acid: A major source of OH radicals in a forest, Geophys. Res. Lett., 32, L05818, doi:10.1029/2005GL022524, 2005.

Kossmann, M., Vogtlin, R., Corsmeier, U., Vogel, B., Fiedler, F., Binder, H. J., Kalthoff, N., and Beyrich, F.: Aspects of the convective boundary layer structure over complex terrain, Atmos. Eniviron., 32, 1323–1348, 1998.

Kramm, G., Muller, H., Fowler, D., Hofken, K. D., Meixner, F. X., and Schaller, E.: A Modified Profile Method for Determining the Vertical Fluxes of NO, NO_2, Ozone, and HNO_3 in the Atmospheric Surface-Layer, J. Atmos. Chem., 13, 265–288, 1991.

Kramm, G., Dlugi, R., Dollard, G. J., Foken, T., Molders, N., Muller, H., Seiler, W., and Sievering, H.: On the Dry Deposition of Ozone and Reactive Nitrogen Species, Atmos. Eniviron., 29, 3209–3231, 1995.

Kroll, J. H., Hanisco, T. F., Donahue, N. M., Demerjian, K. L., and Anderson, J. G.: Accurate, direct measurements of OH yields from gas-phase ozone-alkene reactions using an in situ LIF instrument, Geophys. Res. Lett., 28, 3863–3866, 2001.

Kroll, J. H., Ng, N. L., Murphy, S. M., Flagan, R. C., and Seinfeld, J. H.: Secondary organic aerosol formation from isoprene photooxidation under high-NO_x conditions, Geophys. Res. Lett., 32, L18808, doi:10.1029/2005GL023637, 2005.

Kurpius, M. R. and Goldstein, A. H.: Gas-phase chemistry dominates O_3 loss to a forest, implying a source of aerosols and hydroxyl radicals to the atmosphere, Geophys. Res. Lett., 30, 1371–1375, doi:10.1029/2002GL016785, 2003.

Lamanna, M. S. and Goldstein, A. H.: In situ measurements of C_2-C_{10} volatile organic compounds above a Sierra Nevada ponderosa pine plantation, J. Geophys. Res., 104, 21 247–21 262, 1999.

Larsen, B. R., Di Bella, D., Glasius, M., Winterhalter, R., Jensen, N. R., and Hjorth, J.: Gas-phase OH oxidation of monoterpenes: Gaseous and particulate products, J. Atmos. Chem., 38, 231–276, 2001.

Lee, A., Goldstein, A. H., Keywood, M. D., Gao, S., Varutbangkul, V., Bahreini, R., Ng, N. L., Flagan, R. C., and Seinfeld, J. H.: Gas-phase products and secondary aerosol yields from the ozonolysis of ten different terpenes, J. Geophys. Res., 111, D07302, doi:10.10.1029/2005JD006437, 2006.

Lefer, B. L., Talbot, R. W., and Munger, J. W.: Nitric acid and ammonia at a rural northeastern U.S. site, J. Geophys. Res., 104, 1645–1662, 1999.

Lelieveld, J., van Aardenne, J., Fischer, H., de Reus, M., Williams, J., and Winkler, P.: Increasing ozone over the Atlantic Ocean, Science, 304, 1483–1487, 2004.

Madronich, S. and Flocke, S.: The role of solar radiation in atmospheric chemistry, in *Handbook of Environmental Chemistry*, edited by Boule, P., Springer-Verlag, Heidelberg, 1998.

Martens, C. S., Shay, T. J., Mendlovitz, H. P., Matross, D. M., Saleska, S. R., Wofsy, S. C., Woodward, W. S., Menton, M. C., De Moura, J. M. S., Crill, P. M., De Moraes, O. L. L., and Lima, R. L.: Radon fluxes in tropical forest ecosystems of Brazilian Amazonia: night-time CO2 net ecosystem exchange derived from radon and eddy covariance methods, Global Change Biology, 10, 618–629, 2004.

Meyers, T. P., Huebert, B. J., and Hicks, B. B.: HNO_3 Deposition to a Deciduous Forest, Bound.-Lay. Meteorol., 49, 395–410, 1989.

Munger, J. W., Wofsy, S. C., Bakwin, P. S., Fan, S.-M., Goulden, M. L., Daube, B. C., Goldstein, A. H., Moore, K. E., and Fitzjarrald, D. R.: Atmospheric deposition of reactive nitrogen oxides and ozone in a temperate deciduous forest and a subarctic woodland. 1. Measurements and mechanisms, J. Geophys. Res., 101, 12 639–12 657, 1996.

Murphy, J. G., Day, D. A., Cleary, P. A., Wooldridge, P. J., and Cohen, R. C.: Observations of the diurnal and seasonal trends in nitrogen oxides in the western Sierra Nevada, Atmos. Chem. Phys., 6, 5321–5338, 2006a, http://www.atmos-chem-phys.net/6/5321/2006/.

Murphy, J. G., Day, D. A., Cleary, P. A., Wooldridge, P. J., Millet, D. B., Goldstein, A., and Cohen, R. C.: The weekend effect within and downwind of Sacramento: Part 1. Observations of ozone, nitrogen oxides, and VOC reactivity, Atmos. Chem. Phys. Discussions, 6, 11 427–11 464, 2006b.

Murphy, J. G., Day, D. A., Cleary, P. A., Wooldridge, P. J., Millet, D. B., Goldstein, A. H., and Cohen, R. C.: The weekend effect within and downwind of Sacramento: Part 2. Observational evidence for chemical and dynamical contributions, Atmos. Chem. Phys. Discuss., 6, 11 971–12 019, 2006c.

Neftel, A., Blatter, A., Hesterberg, R., and Staffelbach, T.: Measurements of concentration gradients of HNO_2 and HNO_3 over a semi-natural ecosystem, Atmos. Eniviron., 30, 3017–3025, 1996.

Nemitz, E., Sutton, M. A., Wyers, G. P., and Jongejan, P. A. C.: Gas-particle interactions above a Dutch heathland: 1. Surface exchange fluxes of NH_3, SO_2, HNO_3 and HCl, Atmos. Chem. Phys., 4, 989–1005, 2004, http://www.atmos-chem-phys.net/4/989/2004/.

Neuman, J. A., Huey, L. G., Ryerson, T. B., and Fahey, D. W.: Study of inlet materials for sampling atmospheric nitric acid, Environ. Sci. Technol., 33, 1133–1136, 1999.

Nielsen, O. J., Sidebottom, H. W., Donlon, M., and Treacy, J.: Rate constants for the gas-phase reactions of OH radicals and Cl atoms with normal-alkyl nitrites at atmospheric-pressure and 298-K, Int. J. Chem. Kinet., 23, 1095–1109, 1991.

O'Brien, J. M., Shepson, P. B., Muthuramu, K., Hao, C., Niki, H., Hastie, D. R., Taylor, R., and Roussel, P. B.: Measurements of Alkyl and Multifunctional Organic Nitrates at a Rural Site in Ontario, J. Geophys. Res., 100, 22 795–22 804, 1995.

O'Brien, J. M., Czuba, E., Hastie, D. R., Francisco, J. S., and Shepson, P. B.: Determination of the hydroxy nitrate yields from the reaction of C_2-C_6 alkenes with OH in the presence of NO, J. Phys. Chem. A, 102, 8903–8908, 1998.

Paulson, S. E. and Orlando, J. J.: The reactions of ozone with alkenes: An important source of HO_x in the boundary layer, Geophys. Res. Lett., 23, 3727–3730, 1996.

Perez, I., Wooldridge, P., and Cohen, R. C.: Laboratory evaluation of a novel thermal dissociation chemiluminescence method for in situ detection of nitrous acid, Atmos. Eniviron., 41, 3993–4001, 2007.

Poschl, U., von Kuhlmann, R., Poisson, N., and Crutzen, P. J.: Development and intercomparison of condensed isoprene oxidation mechanisms for global atmospheric modeling, J. Atmos. Chem., 37, 29–52, 2000.

Pryor, S. and Klemm, O.: Experimentally derived estimates of nitric acid dry deposition velocity and viscous sub-layer resistance at a conifer forest, Atmos. Eniviron., 38, 2769–2777, 2004.

Pryor, S. C., Barthelmie, R. J., Jensen, B., Jensen, N. O., and Sorensen, L. L.: HNO_3 fluxes to a deciduous forest derived using gradient and REA methods, Atmos. Eniviron., 36, 5993–5999, 2002.

Raivonen, M., Bonn, B., Sanz, M., Vesala, T., Kulmala, M. and Hari, P.: UV-induced NO_y emissions from Scots pine: Could they originate from photolysis of deposited HNO_3?, Atmos. Eniviron., 40, 6201–6213, 2006.

Ren, X., Olson, J. R., Crawford, J. H., Brune, W. H., Mao, J., Long, R. B., Chen, G., Avery, M. A., Sachse, G. W., Barrick, J. D., Diskin, G. S., Huey, L. G., Fried, A., Cohen, R. C., Heikes, B., Wennberg, P., Singh, H. B., Blake, D. R., and Shetter, R. E.: HO_x Observation and Model Comparison during INTEX-A 2004, J. Geophys. Res., 113, D05310, doi:10.1029/2007JD009166, 2008.

Rinne, J., Taipale, R., Markkanen, T., Ruuskanen, T. M., Hellén, H., Kajos, M. K., Vesala, T., and Kulmala, M.: Hydrocarbon fluxes above a Scots pine forest canopy: measurements and modeling, Atmos. Chem. Phys., 7, 3361–3372, 2007, http://www.atmos-chem-phys.net/7/3361/2007/.

Rondon, A., Johansson, C., and Granat, L.: Dry Deposition of Nitrogen-Dioxide and Ozone to Coniferous Forests, J. Geophys. Res., 98, 5159–5172, 1993.

Rondon, A. and Granat, L.: Studies on the Dry Deposition of NO_2 to Coniferous Species at Low NO_2 Concentrations, Tellus B, 46, 339–352, 1994.

Rosen, R. S., Wood, E. C., Wooldridge, P. J., Thornton, J. A., Day, D. A., Kuster, W., Williams, E. J., Jobson, B. T., and Cohen, R. C.: Observations of total alkyl nitrates during Texas Air Quality Study 2000: Implications for O_3 and alkyl nitrate photochemistry, J. Geophys. Res., 109, D07303, doi:10.1029/2003JD004227, 2004.

Rummel, U., Ammann, C., Gut, A., Meixner, G. X., and Andreae, M. O.: Eddy covariance measurements of nitric oxide flux within an Amazonian rain forest, J. Geophys. Res., 107, 8050, doi:10.1029/2001JD000520, 2002.

Sander, S. P., Finlayson-Pitts, B. J., Friedl, R. R., Golden, D. M., Huie, R. E., Keller-Rudek, H., Kolb, C. E., Kurylo, M. J., Molina, M. J., Moortgat, G. K., Orkin, V. L., Ravishankara, A. R., and Wine, P. H.: Chemical Kinetics and Photochemical Data for Use in Atmospheric Studies, Evaluation Number 15, in JPL Publication 06-2, Jet Propulsion Laboratory, Pasadena, 2006.

Schade, G. W. and Goldstein, A. H.: Fluxes of oxygenated volatile organic compounds from a ponderosa pine plantation, J. Geophys. Res., 106, 3111–3123, 2001.

Schlessinger, W.: Biogeochemistry: an analysis of global change, 588 pp., Academic Press, San Diego, 1997.

Schrimpf, W., Lienaerts, K., Muller, K. P., Rudolph, J., Neubert, R., Schubler, W., and Levin, I.: Dry deposition of peroxyacetyl

nitrate (PAN): Determination of its deposition velocity at night from measurements of the atmopsheric PAN and ^{222}Radon concentration gradient, Geophys. Res. Lett., 23, 3599–3602, 1996.

Seaman, N. L., Stauffer, D. R., and Lariogibbs, A. M.: A Multiscale 4-Dimensional Data Assimilation System Applied in the San-Joaquin Valley During SARMAP .1. Modeling Design and Basic Performance-Characteristics, J. Appl. Meteorol., 34, 1739–1761, 1995.

Shepson, P. B., Bottenheim, J. W., Hastie, D. R., and Venkatram, A.: Determination of the Relative Ozone and PAN Deposition Velocities at Night, Geophys. Res. Lett., 19, 1121–1124, 1992.

Shepson, P. B., Mackay, E., and Muthuramu, K.: Henry's law constants and removal processes for several atmospheric beta-hydroxy alkyl nitrates, Environ. Sci. Technol., 30, 3618–3623, 1996.

Shu, Y. G. and Atkinson, R.: Rate Constants for the Gas-Phase Reactions of O_3 with a Series of Terpenes and OH Radical Formation from the O_3 Reactions with Sesquiterpenes at 296+/–2 K, Int. J. Chem. Kinet., 26, 1193–1205, 1994.

Sievering, H., Kelly, T., McConville, G., Seibold, C., and Turnipseed, A.: Nitric acid dry deposition to conifer forests: Niwot Ridge spruce-fir-pine study, Atmos. Eniviron., 35, 3851-3869, 2001.

Sparks, J. P., Monson, R. K., Sparks, K. L. and Lerdau, M.: Leaf uptake of nitrogen dioxide (NO_2) in a tropical wet forest: implications for tropospheric chemistry, Oecologia, 127, 214–221, 2001.

Stroud, C., Makar, P., Karl, T., Guenther, A., Geron, C., Turnipseed, A., Nemitz, E., Baker, B., Potosnak, M., and Fuentes, J. D.: Role of canopy-scale photochemistry in modifying biogenic-atmosphere exchange of reactive terpene species: Results from the CELTIC field study, J. Geophys. Res., 110, D17303, doi:10.1029/2005JD005775, 2005.

Takemoto, B. K., Bytnerowicz, A., and Fenn, M. E.: Current and future effects of ozone and atmospheric nitrogen deposition on California's mixed conifer forests, Forest Ecology and Management, 144, 159–173, 2001.

Tan, D., Faloona, I., Simpas, J. B., Brune, W., Shepson, P. B., Couch, T. L., Sumner, A. L., Carroll, M. A., Thornberry, T., Apel, E., Riemer, D., and Stockwell, W.: HO_x budgets in a deciduous forest: Results from the PROPHET summer 1998 campaign, J. Geophys. Res., 106, 24 407–24 427, 2001.

Tarnay, L., Gertler, A. W., Blank, R. R., and Taylor Jr., G. E.: Preliminary measurements of summer nitric acid and ammonia concentrations in the Lake Tahoe Basin air-shed: implications for dry deposition of atmospheric nitrogen, Environmental Pollution, 113, 145–153, 2001.

Thornton, J., Wooldridge, P., Cohen, R., Martinez, M., Harder, H., Brune, W., Williams, E., Roberts, J., Fehsenfeld, F., Hall, S., Shetter, R., Wert, B., and Fried, A.: Ozone production rates as a function of NO_x abundances and HO_x production rates in the Nashville urban plume, J. Geophys. Res., 107(D12), 4146, doi:10.1029/JD000932, 2002.

Thornton, J. A., Wooldridge, P. J., and Cohen, R. C.: Atmospheric NO_2: In situ laser-induced fluorescence detection at parts per trillion mixing ratios, Anal. Chem., 72, 528–539, 2000.

Thornton, J. A., Wooldridge, P. J., Cohen, R. C., Williams, E. J., Hereid, D. P., Fehsenfeld, F. C., Stutz, J., and Alicke, B.: Comparisons of in situ and long path measurements of NO_2 in urban plumes, J. Geophys. Res., 108, 4496, doi:10.1029/2003JD003559, 2003.

Treves, K. and Rudich, Y.: The atmospheric fate of C_3-C_6 hydroxyalkyl nitrates, J. Phys. Chem. A, 107, 7809–7817, 2003.

Tunved, P., Hansson, H. C., Kerminen, V. M., Strom, J., Dal Maso, M., Lihavainen, H., Viisanen, Y., Aalto, P. P., Komppula, M. and Kulmala, M.: High natural aerosol loading over boreal forests, Science, 312, 261–263, 2006.

Turnipseed, A. A., Huey, L. G., Nemitz, E., Stickel, R., Higgs, J., Tanner, D. J., Slusher, D. L., Sparks, J. P., Flocke, F. and Guenther, A.: Eddy covariance fluxes of peroxyacetyl nitrates (PANs) and NO_y to a coniferous forest, J. Geophys. Res., 111, D09304, doi:10.1029/2005JD006631, 2006.

Tyndall, G. S., Cox, R. A., Granier, C., Lesclaux, R., Moortgat, G. K., Pilling, M. J., Ravishankara, A. R., and Wallington, T. J.: Atmospheric chemistry of small organic peroxy radicals, J. Geophys. Res., 106, 12 157–12 182, 2001.

Van Oss, R., Duyzer, J., and Wyers, P.: The influence of gas-to-particle conversion on measurements of ammonia exchange over forest, Atmos. Eniviron., 32, 465–471, 1998.

Wildt, J., Kley, D., Rockel, A., Rockel, P., and Segschneider, H. J.: Emission of NO from several higher plant species, J. Geophys. Res., 102, 5919–5927, 1997.

Williams, E. J., Hutchison, G. L., and Fehsenfeld, F. C.: NO_x and N_2O emissions from soil, Global Biogeochem. Cycles, 6, 351–388, 1992.

Zhou, X. L., Gao, H. L., He, Y., Huang, G., Bertman, S. B., Civerolo, K., and Schwab, J.: Nitric acid photolysis on surfaces in low-NO_x environments: Significant atmospheric implications, Geophys. Res. Lett., 30, 2217, doi:10.1029/2003GL018620, 2003.